

Analysis of an Electric Vehicle

Rahul A Phatak, Prithvi Chirag Patel, K. S. Sai Sabareesh, Akash Surendran, G N S Surendranadh Chowdary, Swapnil Sawarn, Prathapagiri Chidananda, Neelabh Bhadauria

Motorcycle Geometry

The most important part of motorcycle designing is determining the geometry of the chassis. It results in the overall behavior of the motorcycle. The geometry determines the overall stiffness, aerodynamics, rider position and comfort, and also affects handling, manoeuvrability and responsiveness. The parameters that primarily dictate the geometry include:

The parameters that primarily affect the geometry include :

1. Castor angle (Rake angle)
2. Trail
3. Wheelbase
4. Steering Offset

These parameters give the foundation to our motorcycle geometry. The interdependence of these parameters are given by the following equations:

1. $a = a_n / \cos \epsilon$

Where 'a' is the ground trail, 'ε' represents the rake or castor angle and 'a_n' is the normal trail

2. $b_n = (p + a) \cos \epsilon$

Where 'b_n' is the rear normal trail and 'p' is the wheelbase

3. $a_n = R_f \sin \epsilon - d$

Where 'R_f' is the front wheel radius and 'd' is the steering offset.

Each parameter affects the performance and handling of the motorcycle differently thus there is no optimal value for each parameter. The type of geometry required depends on the characteristics expected from the bike.

1. Castor angle

The caster angle varies according to the type of motorcycle: from 19° (speedway) to 21-24° for competition or sport motorcycles, up to 27-34° for touring motorcycles. From a structural point of view, a very small angle causes notable stress on the fork during braking. Since the front fork is rather deformable, both flexionally and torsionally, small values of the angle will lead to greater stress and therefore greater deformations, which can cause dangerous vibrations in the front assembly (oscillation of the front assembly around the axis of the steering head, called wobble). The value of the caster angle is closely related to the value of the trail. In general, in order to

have a good feeling for the motorcycle's maneuverability, an increase in the caster angle must be coupled with a corresponding increase in the trail. The value of the trail depends on the type of motorcycle and its wheelbase. It ranges from values of 75 to 90 mm in competition motorcycles to values of 90 to 100 mm in touring and sport motorcycles, up to values of 120 mm and beyond in purely touring motorcycles.

2. Trail

If the value of the trail were negative (the contact point in front of the intersection point of the steering head axis with the road plane) and considering that friction force F is always in the opposite direction of the velocity of slippage, a moment around the steering head axis that would tend to increase the rotation to the left would be generated. One can observe how friction force F would amplify the disturbing effect, seriously compromising the motorcycle's equilibrium. The road profile can make the trail negative, for example, when the wheel goes over a step or bump. This is the reason why we avoid having a negative trail value. Since the load on the front wheels is high due to the weight of the motorcycle, the choice of a small trail lowers the value of the torque that the rider must apply to the handlebars to execute a given maneuver. In addition, it is worth pointing out that these motorcycles are normally used at rather low velocities, and they do not therefore need long trails, which, as previously noted, assures a high directional stability at high velocities. The value of the trail depends on the type of motorcycle and its wheelbase. It ranges from values of 75 to 90 mm in competition motorcycles to values of 90 to 100 mm in touring and sport motorcycles, up to values of 120 mm and beyond in purely touring motorcycles.

3. Wheelbase

In general, an increase in the wheelbase, assuming that the other parameters remain constant, leads to:

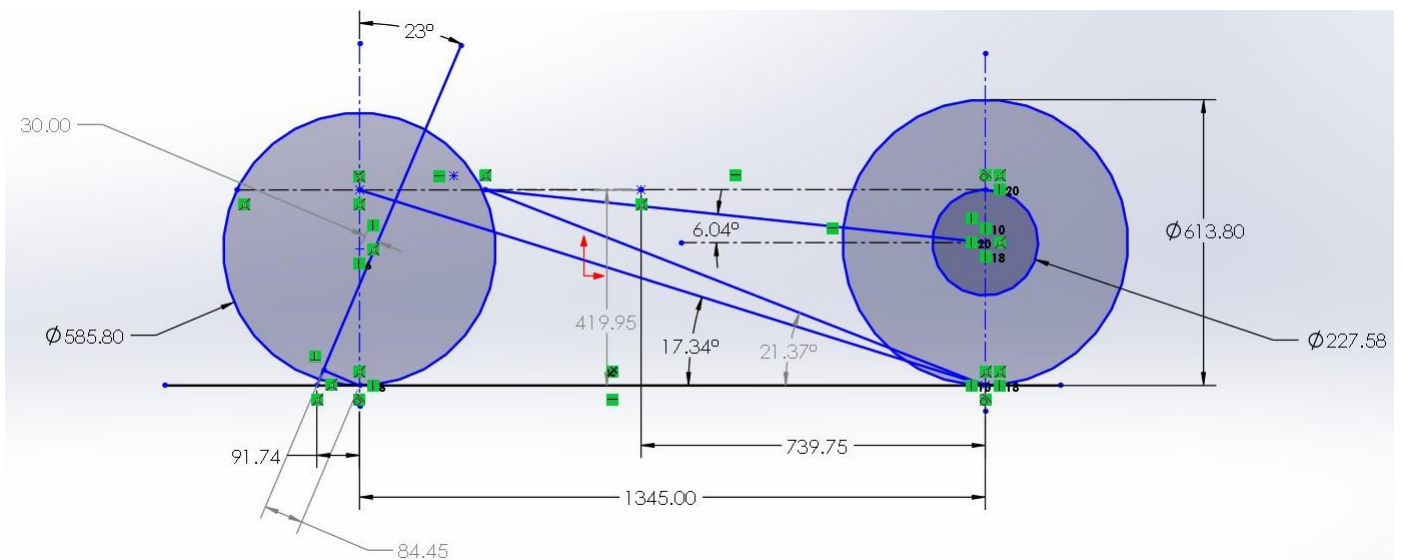
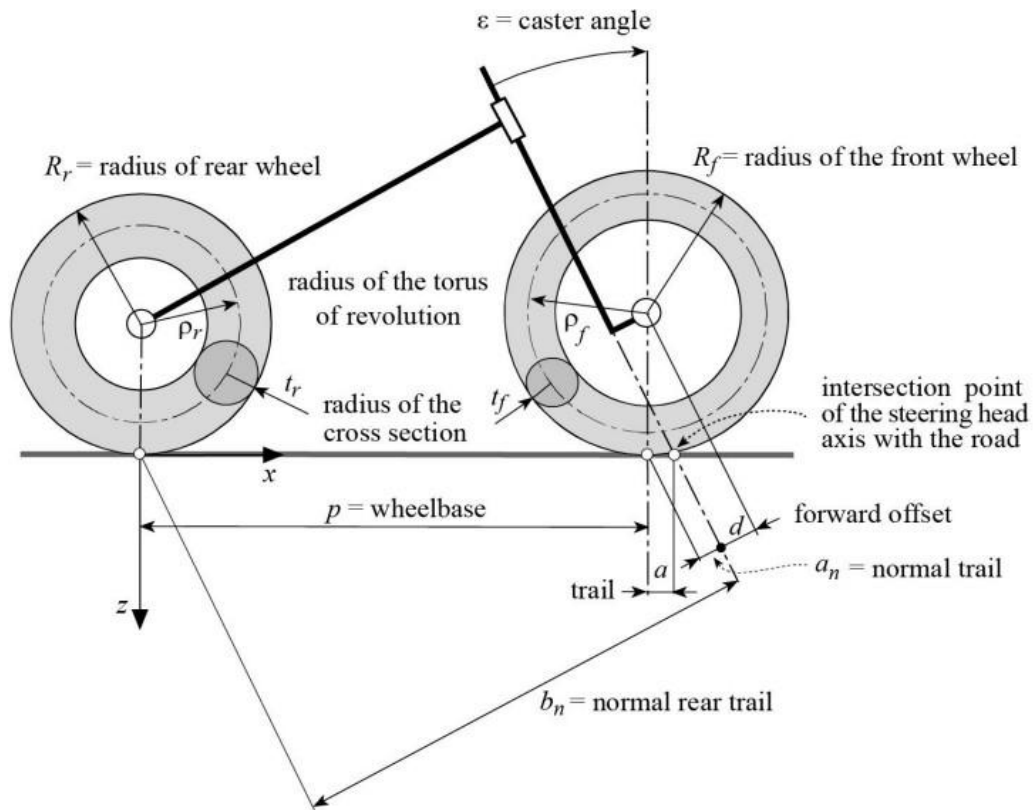
1. An unfavorable increase in the flexural and torsional deformability of the frame. These parameters are very important for maneuverability (frames that are more deformable make the motorcycle less maneuverable).
2. An unfavorable increase in the minimum curvature radius, since it makes it more difficult to turn on a path that has a small curvature radius, in order to turn, there must be an unfavorable increase in the torque applied to the handlebars.
3. A favorable decrease in transferring the load between the two wheels during the acceleration and braking phases, with a resulting decrease in the pitching motion.
4. A favorable reduction in the pitching movement generated by road unevenness
5. A favorable increase in the directional stability of the motorcycle.

The value of the wheelbase varies according to the type of motorcycle. It ranges from 1200 mm in the case of small scooters to 1300 mm for light motorcycles (125 cc displacement) to 1350 mm for medium displacement motorcycles (250 cc) up to 1600 mm, and beyond, for touring motorcycles with greater displacement.

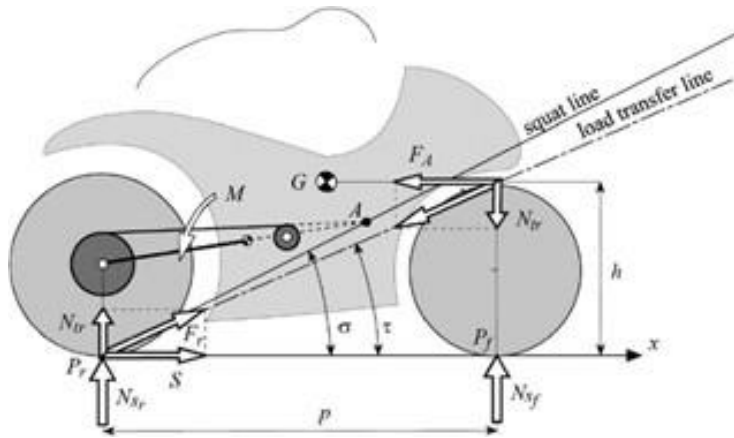
4. Steering Offset

The steering offset is the measurement of the lateral deviation, from the middle of the tyre contact surface, to the trace point. Offset of the wheel spindle from the steering axis is measured at right angles to that axis. With a negative steering offset, (see figure) the track point lies outside of the center, and with positive, inside. If the trace point lies dead center,

its value is zero. Considering the effects of above parameters we conducted multiple iterations to arrive at the ideal vehicle geometry for or prototype.



Squat characteristic



In the rear suspension the squat ratio 'R' is an important parameter to consider as it decides how the rear suspension reacts to the different moments generated, both static and dynamic. We define the squat ratio R as the ratio between the moment generated by the load transfer and the moment generated by the sum of the chain force and the driving force:

$$R = (N_{tr} L \cos \Phi) / (S L \sin \Phi + T L \sin(\Phi - n)) \text{ where}$$

Φ = swingarm angle L = swingarm length

S = moment generated by driving force T = moment generated by chain force N_{tr} = load transfer

n is given by $n = \arcsin[(L \sin \Phi + y_p - (r_c - r_p)) / L_c]$

where y_p is the vertical coordinate of the drive sprocket shaft r_p and r_c represent the radii of the drive sprocket and the rear sprocket, b represents the vertical distance between the axes of the sprockets, L_c is the length of the straight line section of the chain.

Expressing the load transfer as a function of the driving force, the ratio is a function of only the geometric characteristic.

$$R = (h \cos \Phi) / (p [\sin \Phi + R_r \sin(\Phi - n)] / r_c$$

According to the squat ratio three cases can occur:

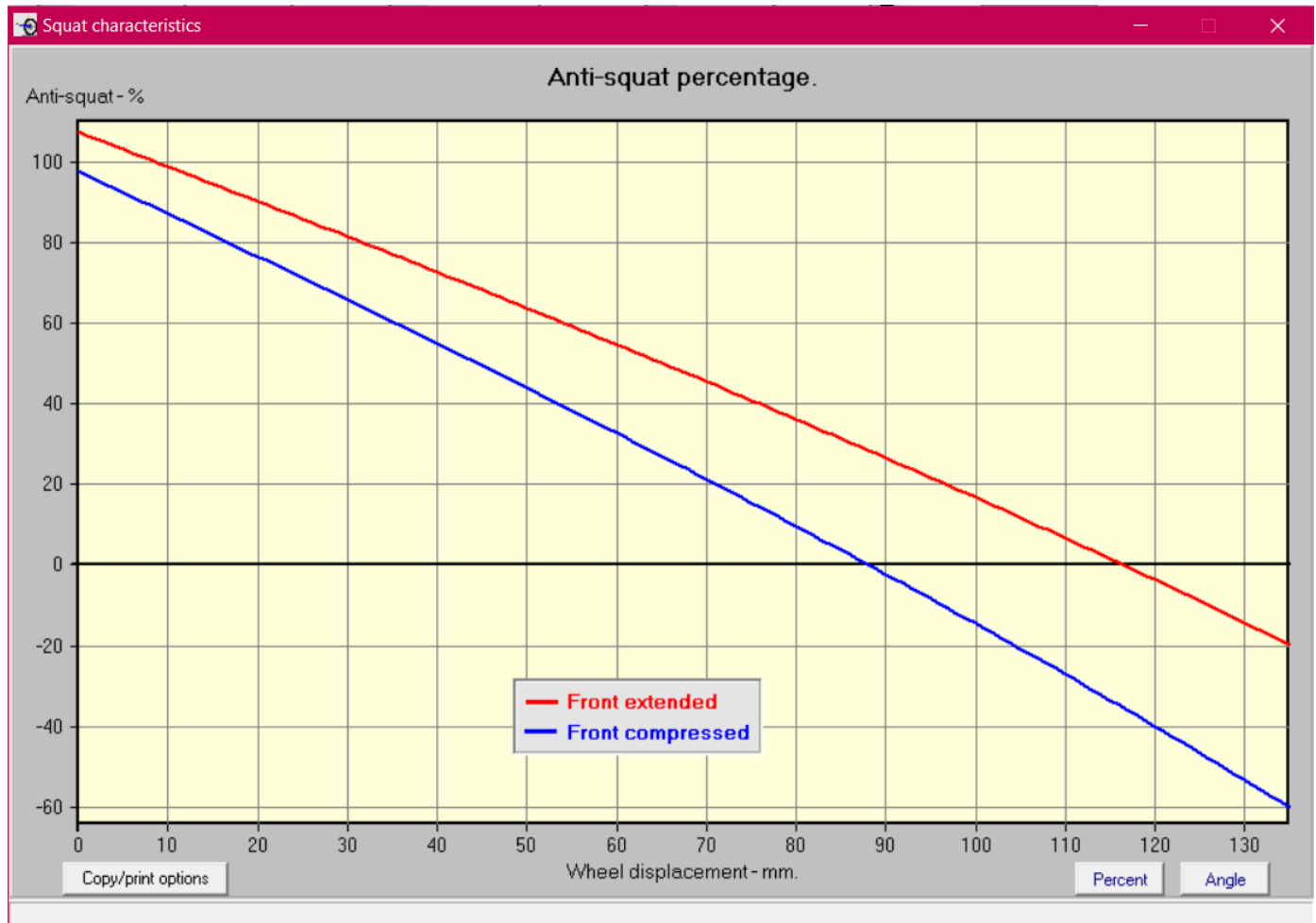
1. Point A lies on the straight line of the load transfer, that is $\sigma = \tau$; in this case $R = 1$. During the thrust phase there are no additional moments operating on the swinging arm, so the suspension spring is no longer stressed compared with the static condition.
2. Point A lies under the straight line of the load transfer, that is $\sigma < \tau$; in this case $R > 1$: the moment generated by the resultant force F_r causes a compression of the spring in addition to the one created by the static load.

3. Point A lies above the straight line of the load transfer, that is $\sigma > \tau$; in this case $R < 1$: The moment generated by the resultant force F_r causes the extension of the spring.

The squat ratio 'R' can also be expressed as $R = \tan \tau / \tan \sigma$ Where,

1. τ (load transfer angle) = 17.34°
2. σ (squat angle) = 21.37°

Therefore $R = 0.79$, and thus $R < 1$, This helps the anti-squat nature of the motorcycle.



Detailed static load cases

As dynamic analysis was not conducted a factor of safety of 1.5 - 2 is favorable as per previous experience to compensate for fatigue and to compensate for random factors a factor of safety of around 2 was considered appropriate.

The following forces act on a motorcycle:

- The weight mg acts at its center of gravity.
- The driving force T , which the ground applies to the motorcycle at the contact point of the rear wheel.

[Type here]

- The vertical reaction forces N_f and N_r exchanged between the tires and the road plane.

Parameter (Unit)	Symbol	Value
Mass of the vehicle (Kg)	m_d	161.07 Kg
Wheelbase (mm)	A	1345
Castor angle (degree)	E	23
Offset (mm)	d	30
Weight distribution (%) (F-R)		55-45
COG to rear (mm)	G_x	739.75
COG height (mm)	G_y	419.95
Max velocity of vehicle (km/hr)	V_{max}	83.33
Radius of rear wheel (mm)	R_r	306.9
Radius of front wheel (mm)	R_f	292.9
Radius of rear sprocket (mm)	R_{crown}	113.788
Max power (W)	P	2000
Swingarm inclination angle (degree)	ϕ	6.04
Angular velocity (m/s)	Ω	22.22

Radius of curvature (m)

 R_c

40

[Type here]

Steering system

Steering is a governing subsystem which is a collection of mechanical linkages to help the rider to guide the vehicle in desired direction or to negotiate a turn along circular pathway. Steering system of a two wheeler involves crucial parameters which determine the stability and manoeuvrability of the vehicle. A steering system for a motorcycle includes a head pipe, a steering stem, a top bridge, a bottom bridge, a front fork, and a steering handlebar.

The motorcycle steering behaviour depends on various geometric parameters:

1. Wheelbase

2. Offset

3. Rake/caster angle

4. Wheel radii

5. Turning angle

6. Roll angle

7. Tire properties (slide slip angles)

The motorcycle steering mechanism for a given offset

When turning the handlebars, keeping the motorcycle perfectly vertical, the steering head lowers and only begins to rise for very high values of the steering angle

The vertical displacement of the wheel centre:

$$\Delta h = R_f \left(1 - \sqrt{1 - \sin^2 \delta \sin^2 \epsilon} \right) - d \cdot \sin \epsilon \cdot (1 - \cos \delta)$$

$$= 0.2929(1 - \sqrt{1 - \sin^2(22^\circ) \sin^2(23^\circ)}) - 0.03(\sin 23^\circ (1 - \cos 22^\circ))$$

$$= 0.002301 \text{ m}$$

Turning Radius

Radius = Wheel base / Sin(90 - Steering angle)

$$= 1.345 / \sin(90 - 22^\circ) = 1.45 \text{ m}$$

Wheel Flip Flop factor:

Wheel flip flop factor = trail * sin(head angle) * cos(head angle)

$$= 91.74 \cdot \sin(67^\circ) \cdot \cos(67^\circ)$$

$$= 32.9 \text{ mm}$$

Motorcycle parameters while in a curve

The motorcycle while going about a steady turn is subjected to two forces i.e the tilting effect (Rolling) and the restoring moment generated by the Centrifugal force that tends to keep the vehicle in a balanced state i.e prevents it from falling into the curve.

Effective Roll Angle:

[Type here]

$$\phi = \phi_i + \Delta\phi = \arctan \frac{V^2}{gR_c} + \arcsin \frac{t \cdot \sin \left(\arctan \frac{V^2}{gR_c} \right)}{h-t}$$

$$= \arctan(23.5^2/9.81*40) + \arcsin(55 * \arctan(23.5^2/9.81*40)/419.95 - 55$$

$$= 60.97 \text{ degrees}$$

V= forward velocity of the motorcycle Ω = Angular yaw rate (yaw velocity)

Rc= the radius of the turn

g= Acceleration due to Gravity (9.81 m/s²) h= Centre of gravity height

2t = Tire thickness (120mm) Yaw velocity:

$$\Omega = V/(Rc)$$

$$= 23.23 / (40)$$

$$= 0.58 \text{ m/s}$$

Where, V= Forward velocity, Rc= Radius of Curve

Lateral Slip (slip angle) :

It is defined as the angle formed by the direction of forward motion and the plane of the wheel. When sideslip angles approach zero, steering is called kinematic steering.

We consider neutral steering condition for which we have taken the values of the camber and cornering coefficients as 0.6 and 12 respectively

Neutral steering : Steering ratio is '1' i.e front slip = rear slip

Front slip angle:

$$\lambda_f \approx \frac{1 - k_{\phi_f}}{k_{\lambda_f}} \phi$$

$$= (1 - 0.8) * 60.97 / 12$$

$$= 1.0161$$

Rear Slip Angle:

$$\lambda_r \approx \frac{1 - k_{\phi_r}}{k_{\lambda_r}} \phi$$

[Type here]

$$=(1-0.8)*60.97/12$$

$$=1.0161$$

while cornering:

Aerodynamic Forces:

$$\text{Drag force} = (d * V^2 * C_x * S) / 2$$

$$= (1.225 * 14.38^2 * 0.5 * (0.6 \times 10^{-6})) / 2$$

$$= 3.79 \times 10^{-5} \text{ N}$$

Where:

d = air density V = velocity

C_x = Drag coefficient

S = Frontal surface area

Vertical Load on tires while cornering:

Front Tire

$$N_f = mg \frac{b}{p} - F_A \frac{h}{p} \cos \phi$$

$$= 161 * 9.81 * (739.75 / 13445) - 78 * (419.95 / 1345) * \cos(60.97)$$

$$= 856.85 \text{ N}$$

Rear Tire

$$N_r = mg \frac{p-b}{p} + F_A \frac{h}{p} \cos \phi$$

$$= 161 * 9.81 * (739.75 / 13445) - (78 * (419.95 / 1345) \cos(60.97))$$

$$= 856.85 \text{ N}$$

Lateral Forces on both tires:

Front tire:

$$= (12 * 1.0161 + 12 * 60.97) * 856.85$$

$$= 637353.47 \text{ N}$$

Rear Tire:

[Type here]

$$=(12*1.0161+12*60.97)*722.55$$

$$=543318.08 \text{ N}$$

Effective steering Angle :

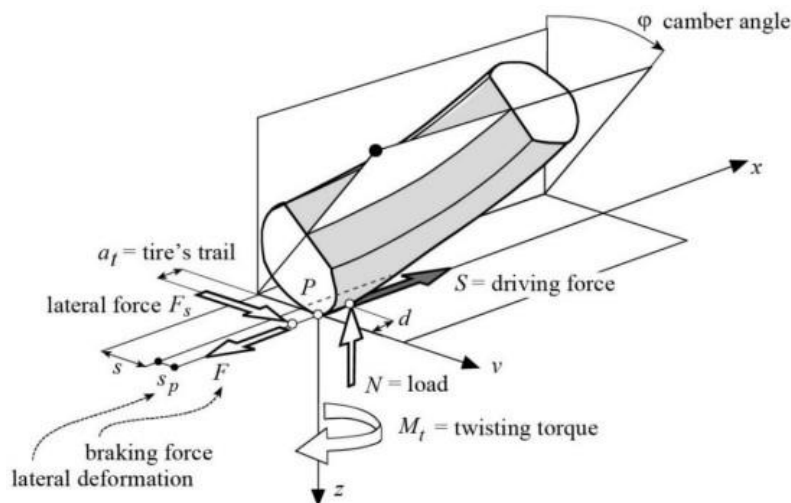
$$\Delta^* = \Delta + \lambda_r - \lambda_f \cong \frac{\cos \epsilon}{\cos \phi} \delta + \lambda_r - \lambda_f$$

$$= \text{Steering angle} + 1.0161 - 1.0161$$

$$= 22 \text{ degrees}$$

Tire Setup

Model of the tire



The model of the motorcycle tire takes into consideration the forces acting on points near the theoretical contact point defined by the tire's geometry.

The forces under consideration are as follows:

1. Normal force: Normal force is applied at a point that precedes, by the distance d , the position of the theoretical contact point.

$$d = fwR = 4.39 \text{ mm}$$

Where, fw = rolling resistance coefficient = 0.015 R = tire's radius = 292.9 mm

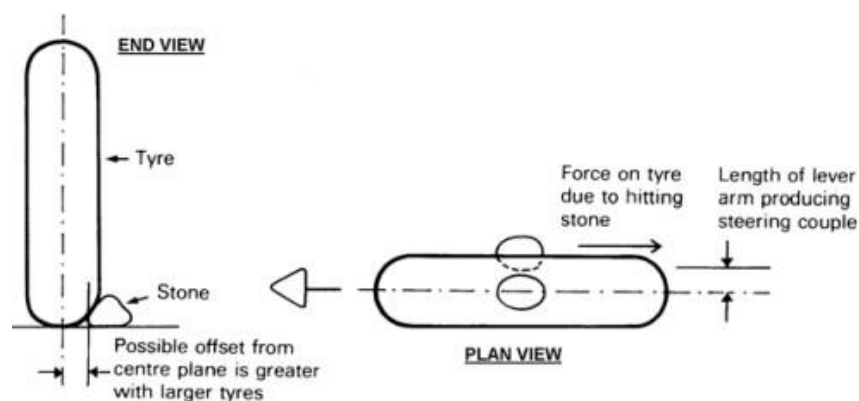
2. Longitudinal force: The force is applied to a point displaced laterally from the theoretical contact point because of the tire's lateral deformability. The lateral displacement s_p , depending on the lateral stiffness of the tire, is generally negligible with respect to the geometric displacement s deriving from the roll inclination of the wheel. The moments acting around the x , y and z -axes are generated by the forces described above and by the twisting moment.

[Type here]

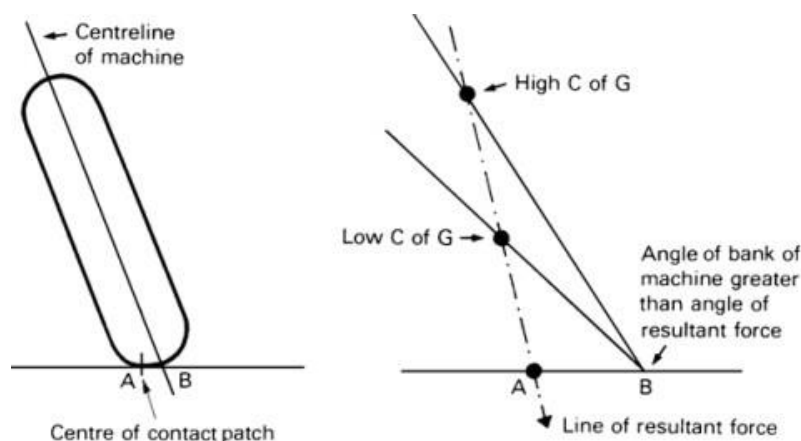
3. Overturning moment: The overturning moment M_x is generated by the vertical load N whose arm is the lateral deformation s_p . $M_x = -s_p N = 1580 \text{ Nmm}$
4. Rolling resistance moment: Rolling resistance moment is generated by the asymmetric distribution of normal stresses that causes a forward displacement of vertical load. The tire's rolling resistance moment is: $M_y = d * N = 4.39 * 161 * 9.81 = 6933.6 \text{ Nmm}$
5. Yawing moment: Yawing moment includes two contributions. The first term, due to the lateral force, tends to align the plane of the tire in the direction of velocity. The second term increases with the camber angle and works against alignment. $M_z = -a_t F_s + M_t$

Factors taken while tire selection:

1. Large tires increase the unsprung mass too, to the detriment of roadholding. Larger tires also increase precessional forces.
2. Road disturbance such as a stone can cause a couple tending to steer the wheel to that side. A wide tire is found by more stones and produces a higher couple.



3. Wide tires may impair handling and stability, even though grip may be improved. The contact patch moves away from the centre plane of the wheel or the steering axis as the machine is banked. A greater angle of lean is necessary to balance centrifugal force, and this may require a slightly higher centre of gravity to restore cornering clearance.



It was decided to go with a of following tire profiles:1. Front - 110/70 R17

[Type here]

2. Rear - 130/70 R17

The tires selected are Michelin pilot street radial tires and comply with requirements specified in AIS:044 (Part 1 to 3) : 2004 as applicable till the corresponding BIS specifications are notified under the Bureau of Indian Standards Act, 1863 (63 of 1986).

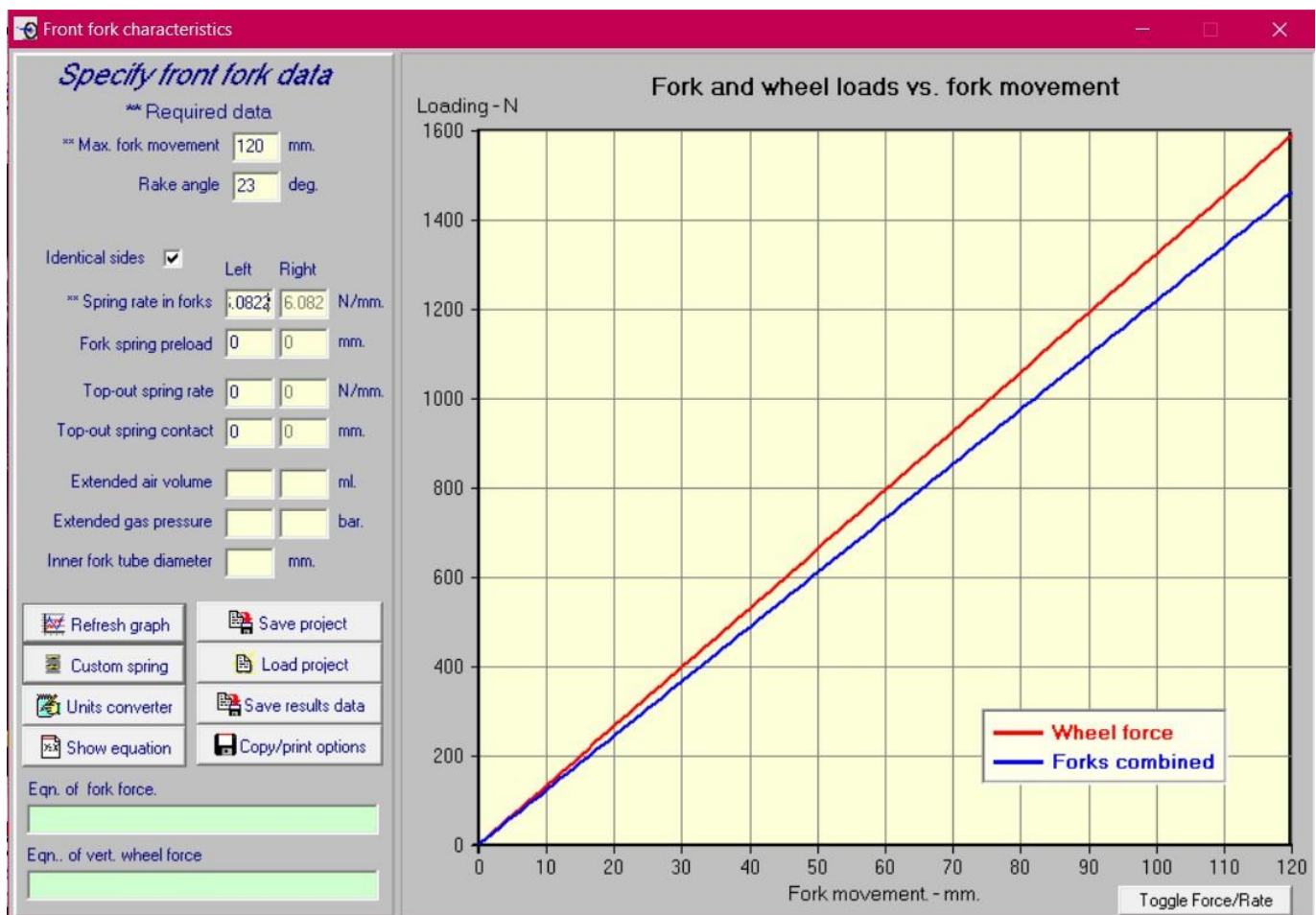
Suspension setup

Front Suspension

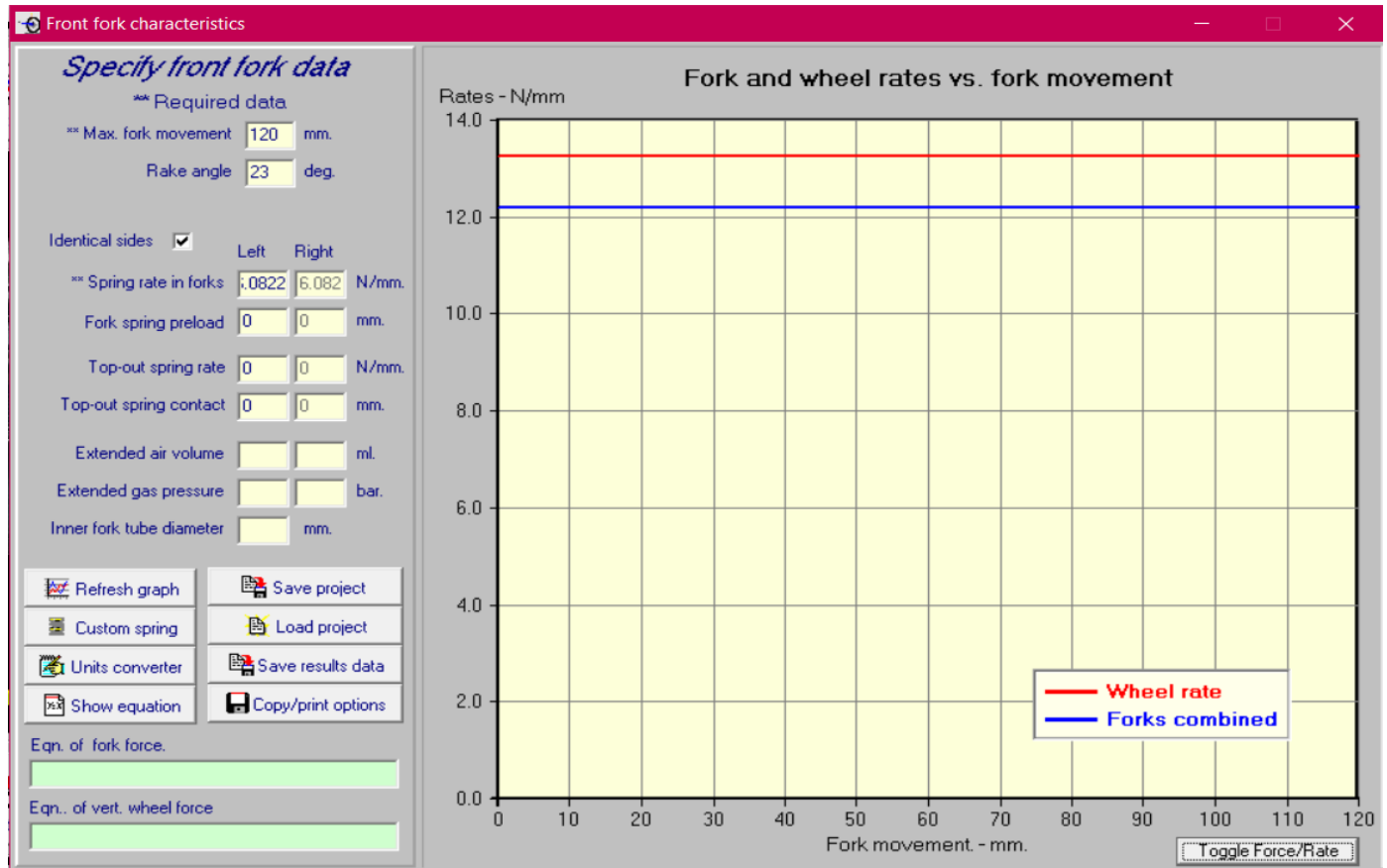
Primarily there are two types of front suspension. Telescopic suspension are the most common front suspension systems, and an overwhelming majority of motorcycles the world over uses this system. A more modern version of the conventional telescopic fork suspension is the upside-down forks, where the sliders, which typically are at the bottom, are positioned at the top. While it offers more stability they are mainly suited for performance oriented machines. Therefore we decided to go for a telescopic suspension of KTM Duke 125. Motochassis (Tony Foyale) software is used for suspension analysis.

Technical data

Fork stroke length= 142 mm Fork length = 744 mm Spring rate = 6.0822 N/mm



[Type here]



Rear Suspension

Primarily there are two types of rear suspension that can be found in a two-wheeler.

1. Dual suspension

S NO.	Advantages	Disadvantages
1	Load bearing capacity of dual suspension is more.	Tuning has to be done in dual suspension
2	If one of the shock absorbers leaks oil then the other can still carry the load.	Adjustment is difficult on the vehicle frame.
3	Cost of dual suspension is less.	Does not provide proper cornering.

[Type here]

4	Maintenance of dual suspension is easy as compared to mono shocks.	Ride is compromised at high speed.
---	--	------------------------------------

2. Mono suspension

S NO.	Advantages	Disadvantages
1	Mono shock eliminate torque to the swing arm and improve braking and handling of vehicle	Cost of ownership and maintenance is high
2	Easier to adjust on the vehicle as there is only one shock to adjust	May get failed if excess load applied
3	The linkage used to connect the shock to the swing arm are frequently designed to give a rising rate of damping for the rear	
4	It has better cornering ability	

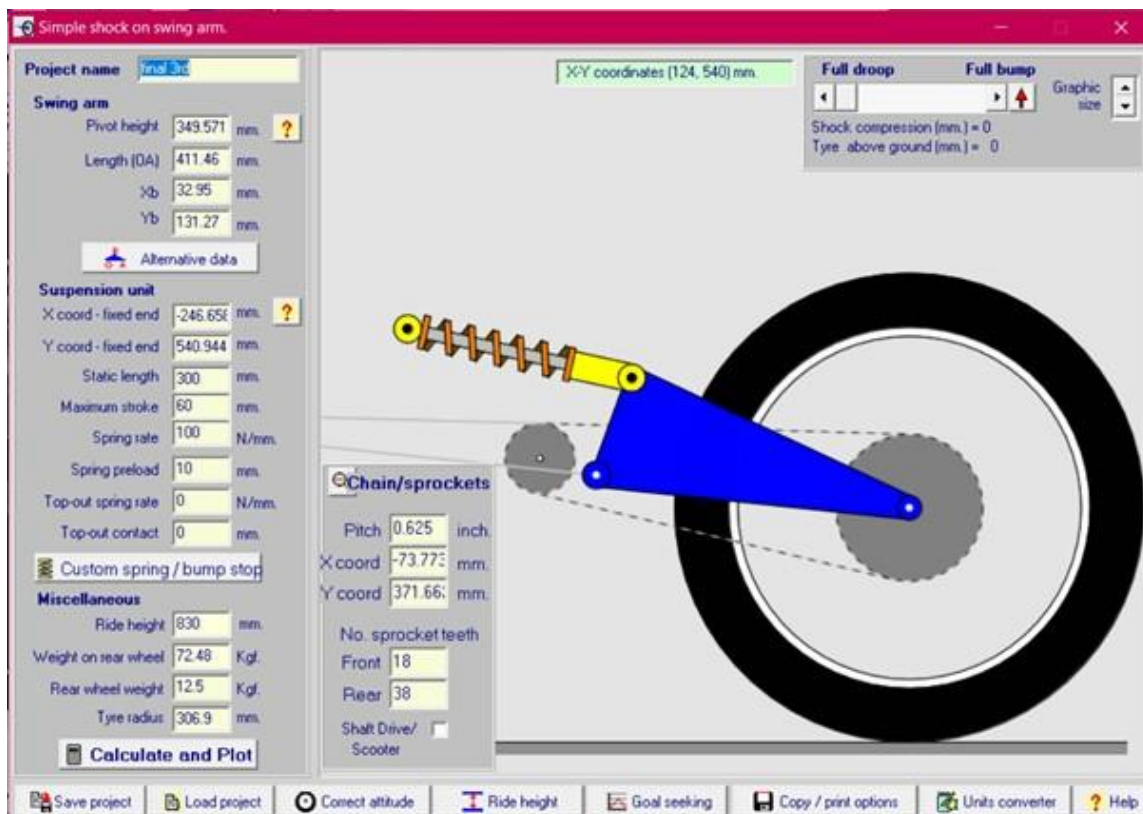
We concluded that mono suspension is superior to dual suspension systems and decided to go with a mono suspension for our prototype. Taking vehicle parameters into consideration we have decided to go with a KTM 390 duke rear mono shock suspension.

Regressive suspension action becomes more useful as it goes deeper into its travel. Regressive bikes tend to run less sag, pedal extremely well, but bottom out easily on larger impacts. After a lot of iterations, we have found the best Suspension mounting points with characteristics like highspeed stability, stability during cornering and leaning. It is hard and stiff suspension as it has lesser sag. Motochassis (Tony Foyale) software is used for suspension analysis.

Suspension Specifications

Specifications	Value
Length	300 mm
Stroke	63 mm
Rebound	35 clicks
Spring preload	10 mm
Spring rate	100 N/mm
Rec. rear sag (R1-R3)	42 mm

Suspension Setup:

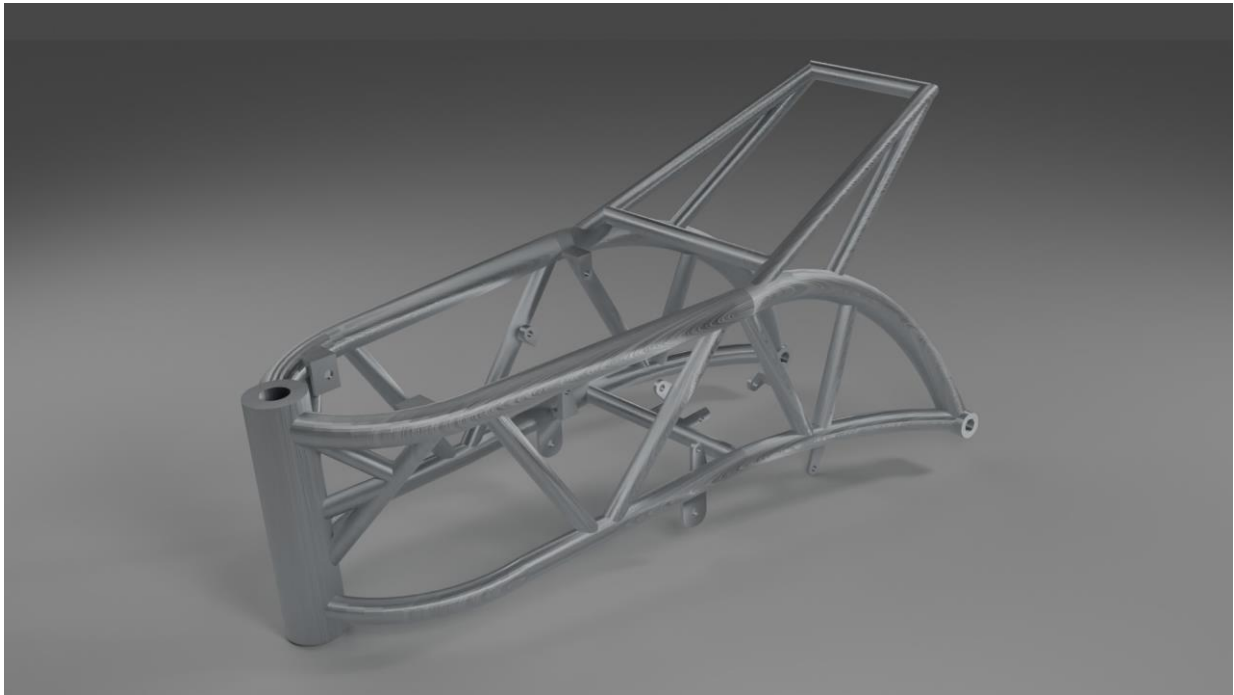


Result:



[Type here]

Chassis



1. Motorcycle frame

The most important part of motorcycle designing is determining the geometry of the motorcycle frame. It results in the overall behaviour of the motorcycle. The basic function of a motorcycle frame is somewhat similar to that of the skeleton in the human body, i.e. to hold together the different parts in one rigid structure. One of the major benefits (for a motorcycle enthusiast) of using an advanced frame design lies in the sporty handling characteristics of the bike. A well-designed frame can add to the joy of riding a motorcycle as the bike would feel more stable, effortless and confident around corners, in straight lines and while braking.

There are varieties of motorcycle frame designs out there, each having its own advantage (for both the manufacturer and the biker/rider). The following options are available for the task:

1. Backbone Frame
2. Single Cradle
3. Double Cradle
4. Perimeter Frame
5. Trellis Frame

On comparing various factors as cost, stiffness and ease of manufacturing, a decision was taken to design a Trellis frame. A motorcycle frame is a structure that must hold the rider while also supporting the battery pack, motor, suspension, steering and all the other components belonging to different systems of the bike. Because of the weight of the parts needed to make the bike function, the frame must be lightweight, inflexible and strong.

Over the years, motorcycle's frames have been made with a variety of materials in an effort to combine strength, agility and nimbleness. Motorcycle frames are usually made of aluminium, steel or alloy with a welding process. Carbon-fibre is used in some expensive or custom frames. Anyway, there are many types of frame materials that could be used to build them but only some of them are really competitive about price, mechanical properties, weight or some other points. The primary focus while selecting the material of a frame is not only to avoid any structural failures in the form cracks or breaks, but also to avoid excessive deformation (elastic or plastic). The material chosen considering the strength, density, availability and machinability was Al7068.

Aluminium is extensively used for automotive chassis and engine applications. Properties like useful strength, low density, high thermal conductivity, excellent machining behaviour and good corrosion resistance are the main reasons for using Aluminium. Electric automobiles need lightweight designing materials like Aluminium because Batteries are heavy. As Aluminium is soft relative to Steel, we look for lesser Equivalent stress rather than Factor of safety.

Properties of AL 7068:

Tensile strength	641 MPa
Yield strength	590 MPa
Young's modulus	73.1 Gpa
Elongation	8%

EXTERNAL FORCES

1. Maximum acceleration

$$\sum f_x = M * a \quad (\text{Eq 1})$$

$$T_{dr} = T * \frac{G_y}{A} \quad (\text{Eq 2})$$

$$\sum f_y = M * a ; \quad (\text{Eq 3})$$

$$N_{dr} - m_d g * \frac{(A - G_x)}{A} = 0; \quad (\text{Eq 4})$$

$$N_{df} - m_d g * \frac{G_x}{A} = 0 \quad (\text{Eq 5})$$

On the rear wheel for diamond chassis $N_r = N_{dr} - T_{dr} = m_d g * \frac{(A - G_x)}{A} - T * \frac{G_y}{A}$ (Eq 6)

On the front wheel for diamond chassis $N_f = N_{df} - T_{dr} = m_d g * \frac{G_x}{A} - T * \frac{G_y}{A}$ (Eq 7)

Knowing that during the maximum acceleration the front wheel or the normal on the front wheel will be approximately neglected.

$$N_f = 0$$

$$N_r = N_{dr} - T_{dr} = m_d g * \frac{(A - G_x)}{A} - T * \frac{G_y}{A}$$

1. Max braking

$$N_{dr} - m_d g * \frac{(A - G_x)}{A} = 0; \quad (\text{Eq 15})$$

$$N_{df} - m_d g * \frac{G_x}{A} = 0 ; \quad \sum f_x = M * a ; T_{dr} = T * \frac{G_y}{A}; \quad (\text{Eq 16})$$

$$\text{On the rear wheel for diamond chassis } N_r = N_{dr} - T_{dr} = m_d g \frac{(A - Gx)}{A} - T \frac{Gy}{A} \quad (\text{Eq 17})$$

$$\text{On the front wheel for diamond chassis } N_f = N_{df} - T_{dr} = m_d g \frac{Gx}{A} - T \frac{Gy}{A} \quad (\text{Eq 18})$$

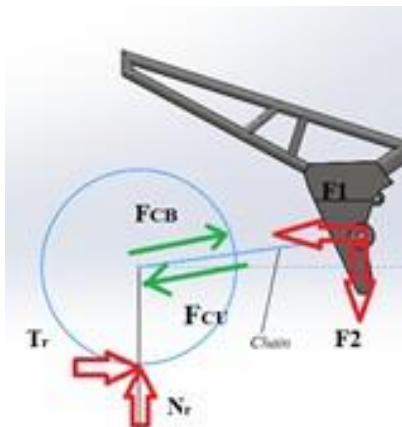
$$N_r = 0$$

$$N_f = m_d g$$

$$T_{df} = m_d g \frac{Gx}{A}$$

INTERNAL FORCES

1. Max acceleration



$$\text{Resolving forces across x and y direction, } T_{dr} - F_1 + F_{cb} \cos(\phi) - F_{cu} \cos(\phi) = 0 \quad (1)$$

$$N_r - F_2 + F_{cb} \sin(\phi) - F_{cu} \sin(\phi) = 0 \quad (2) \quad V_{\max} = 100 \text{ Km/hr} = 27.777 \text{ m/s}$$

$$V_{\max} = W_{\text{wheel}} \cdot R_r$$

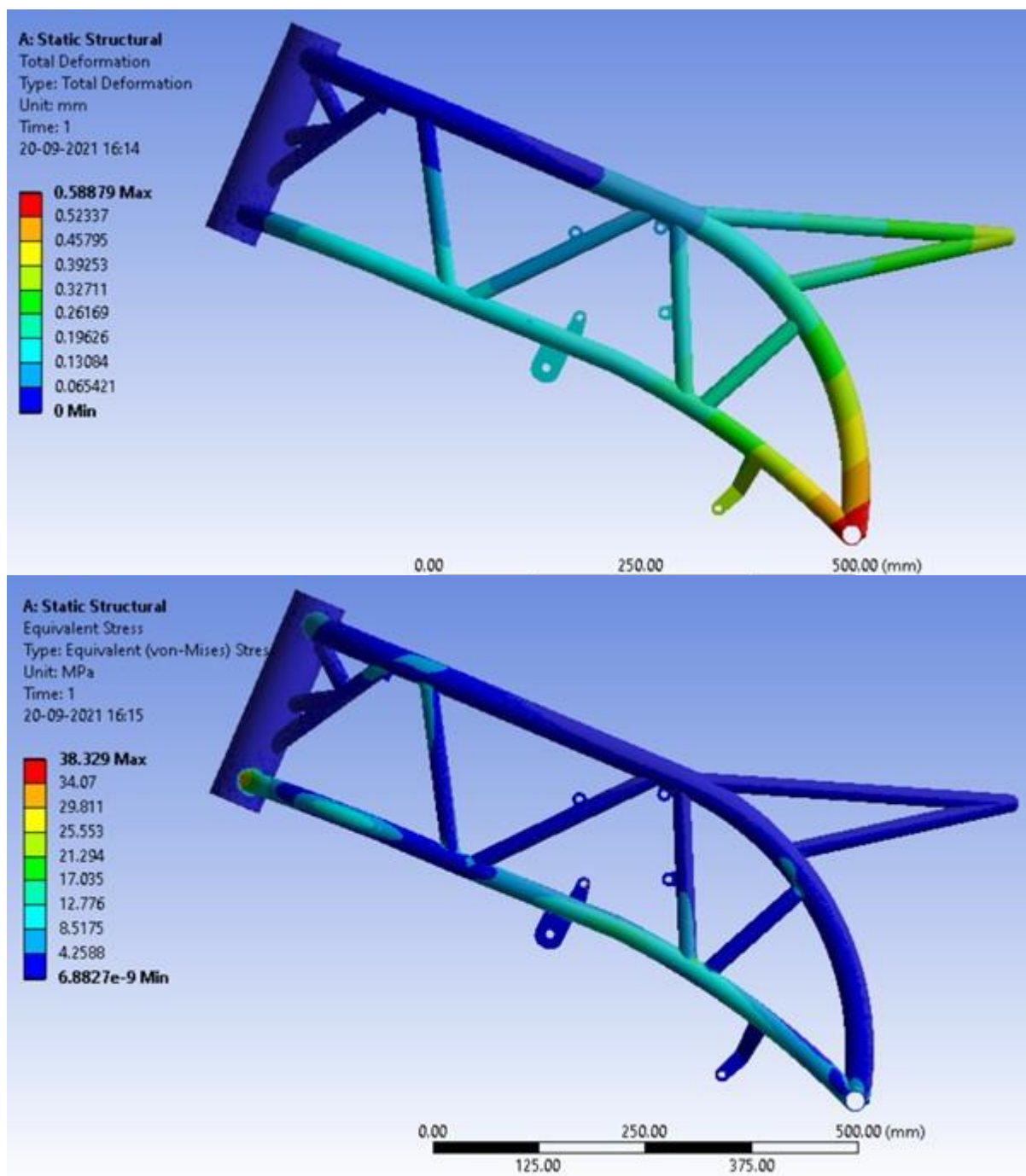
$$W_{\text{wheel}} = V_{\max} / R_r = 27.777 / 0.3059 = 90.80 \text{ rad/s} \quad V_{\text{chain}} = W_{\text{wheel}} \cdot R_{\text{crown}} = 90.80 \cdot 0.113788 = 10.33 \text{ m/s}$$

$$W / V_{\text{chain}} = 2000 / 10.33 = 193.61 \text{ N}$$

$$F_{cu} < F_{cb}$$

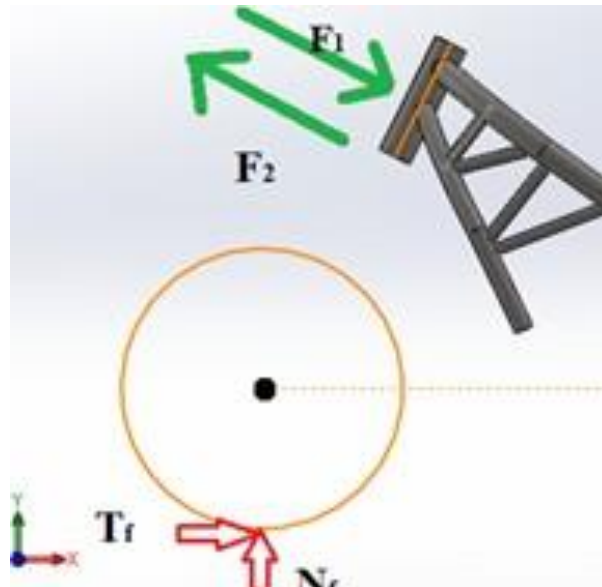
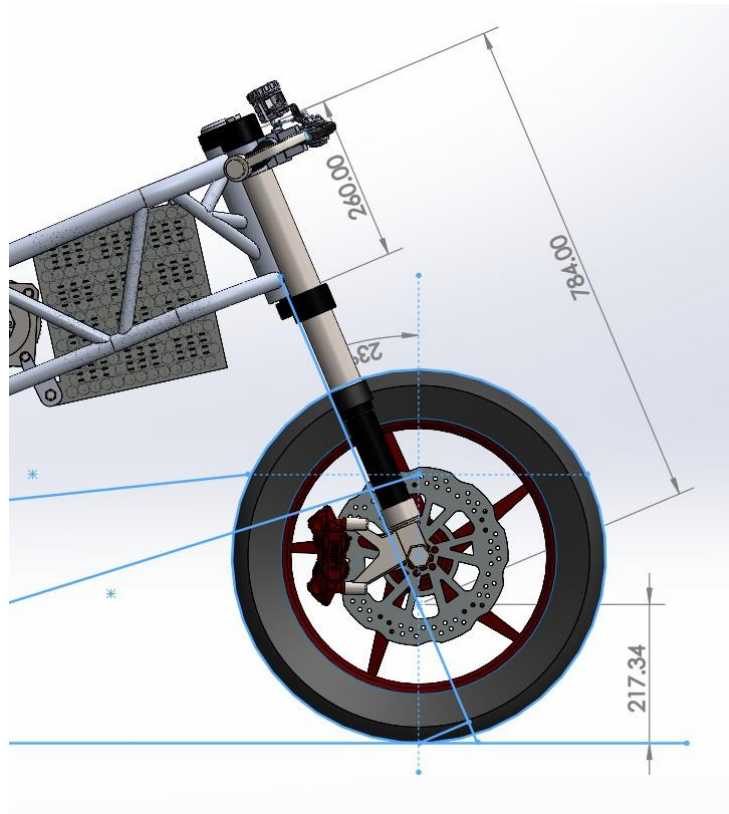
Therefore, $F_{cu} = 150 \text{ N}$ Solving equation we get,

	1 st Iteration	Latest Iteration
F1	2800 N	2321 N
F2	1918 N	1585 N



[Type here]

2. Max braking



$$AB=0.217.34m \quad BC=0.524m \quad CD=0.260m$$

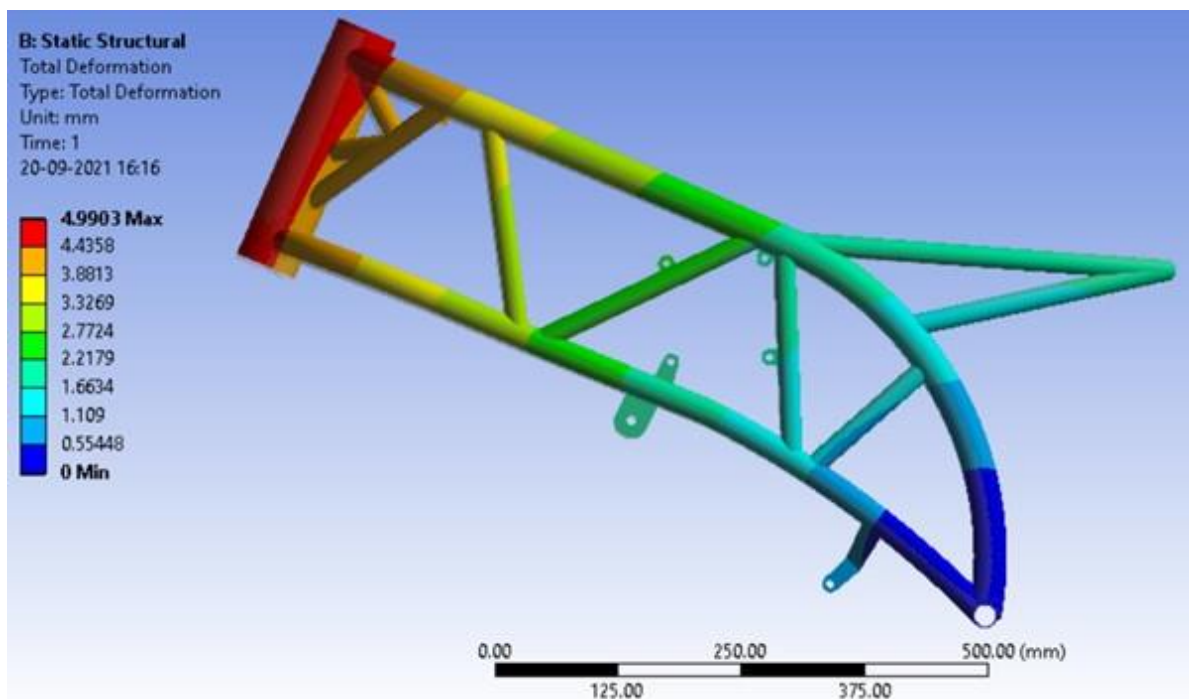
$$Tdf \cdot AB + F2 \cdot BC - BD \cdot F1 = 0$$

[Type here]

$$F2 \cdot CD + Nf \cdot BD \cdot \sin(23) - Tdf \cdot (AB - BD) \cdot \cos(23) = 0;$$

Solving equations we get,

	1 st Iteration	Latest Iteration
F1	4897 N	2651 N
F2	5772 N	3605 N



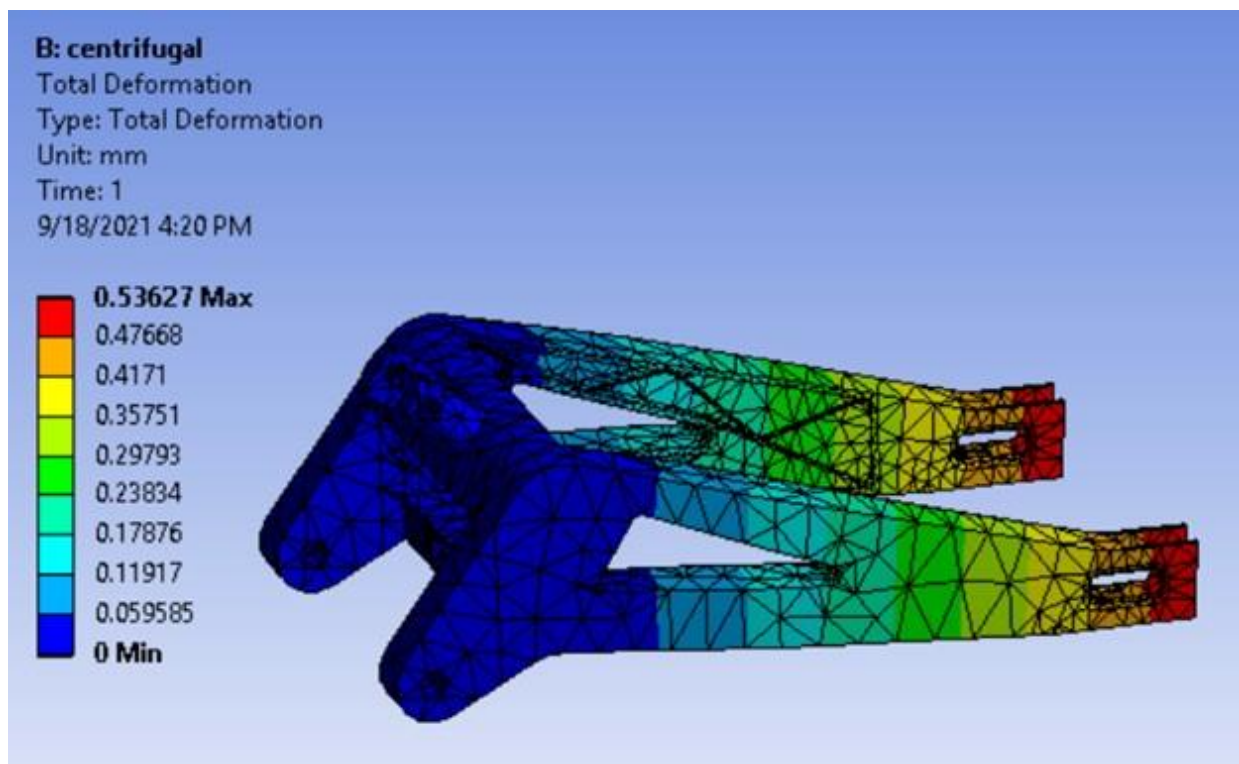
$W = (m \cdot v^2) / r$ Where,

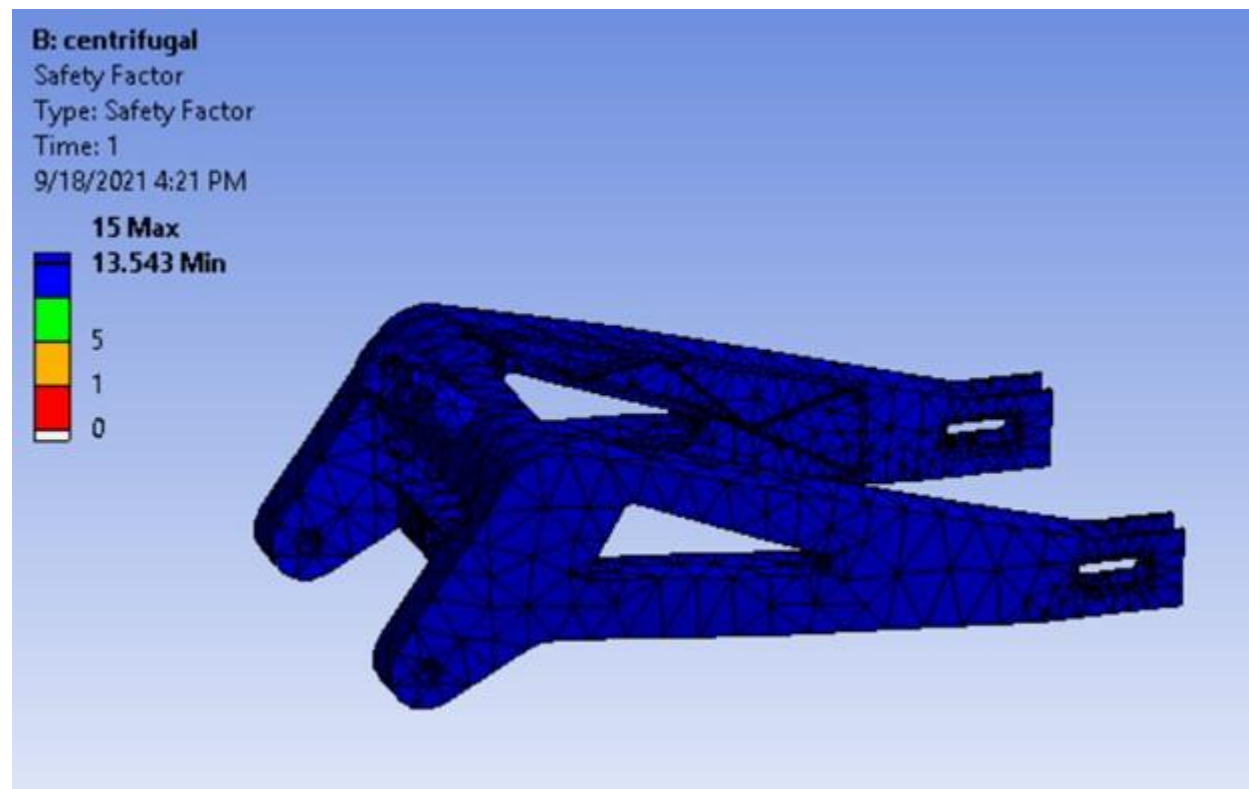
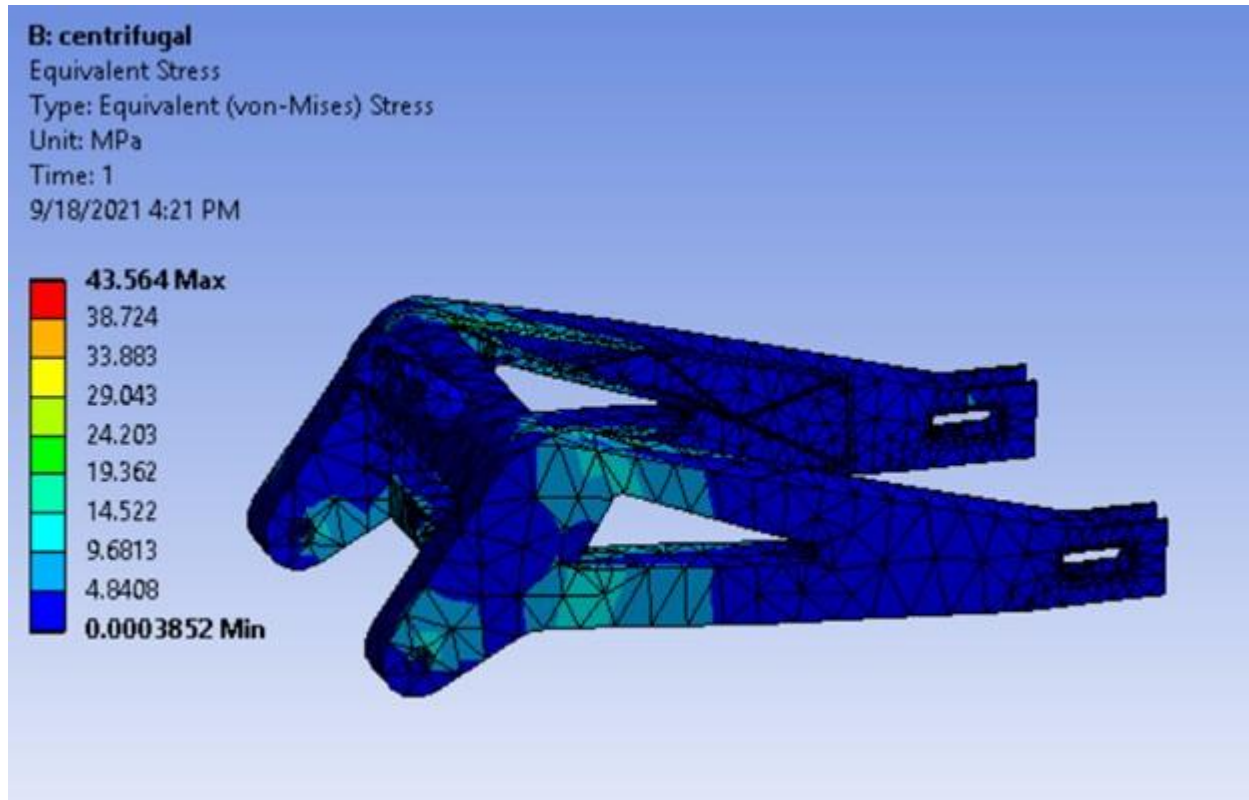
W is centrifugal force, m is net mass, v = max velocity while cornering and r is radius of curvature

We consider the v as 22.22 m/s and r as 40 m $W = (161 \cdot 22.22^2) / 40$

$$W = 1987 \text{ N}$$

S No.	Total Deformation (mm)	Von-Mises stress (Pa)	Factor of safety
1st Iteration	0.37461	31.973	15
2nd Iteration	0.35938	17.102	15
3rd Iteration	0.53627	43.564	13.54

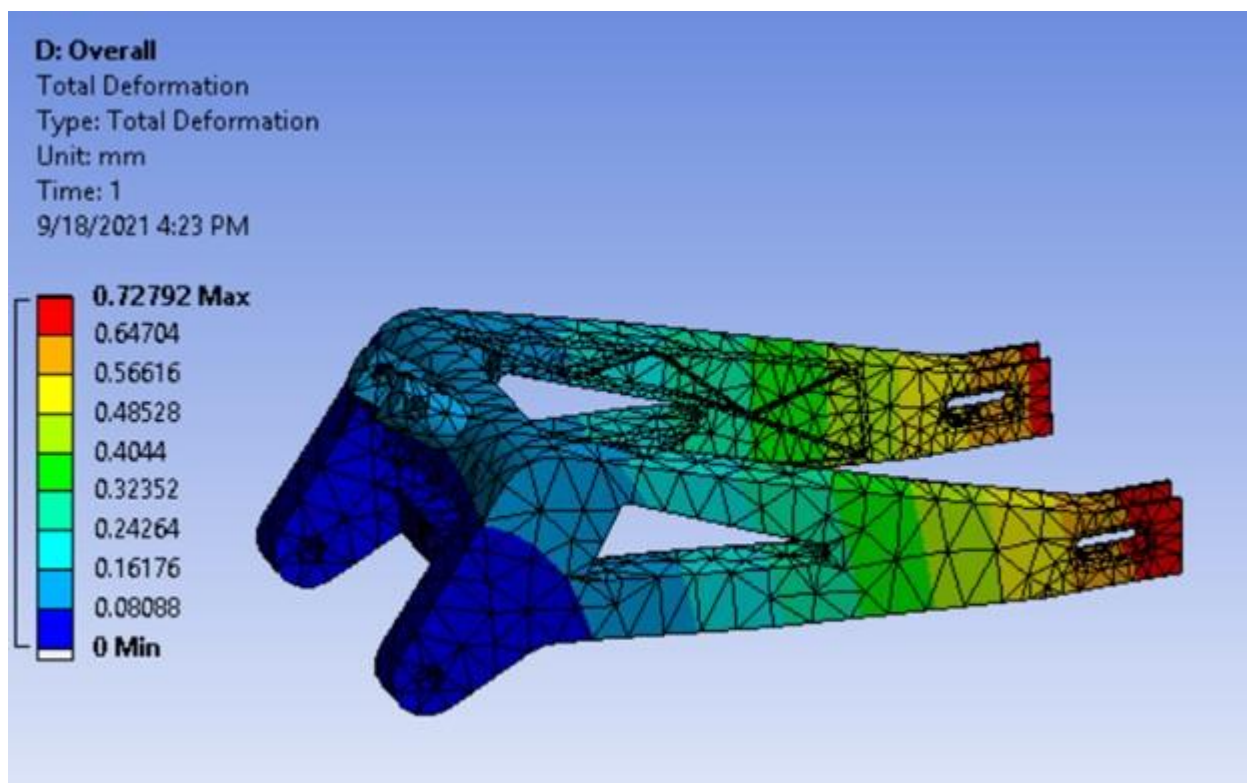


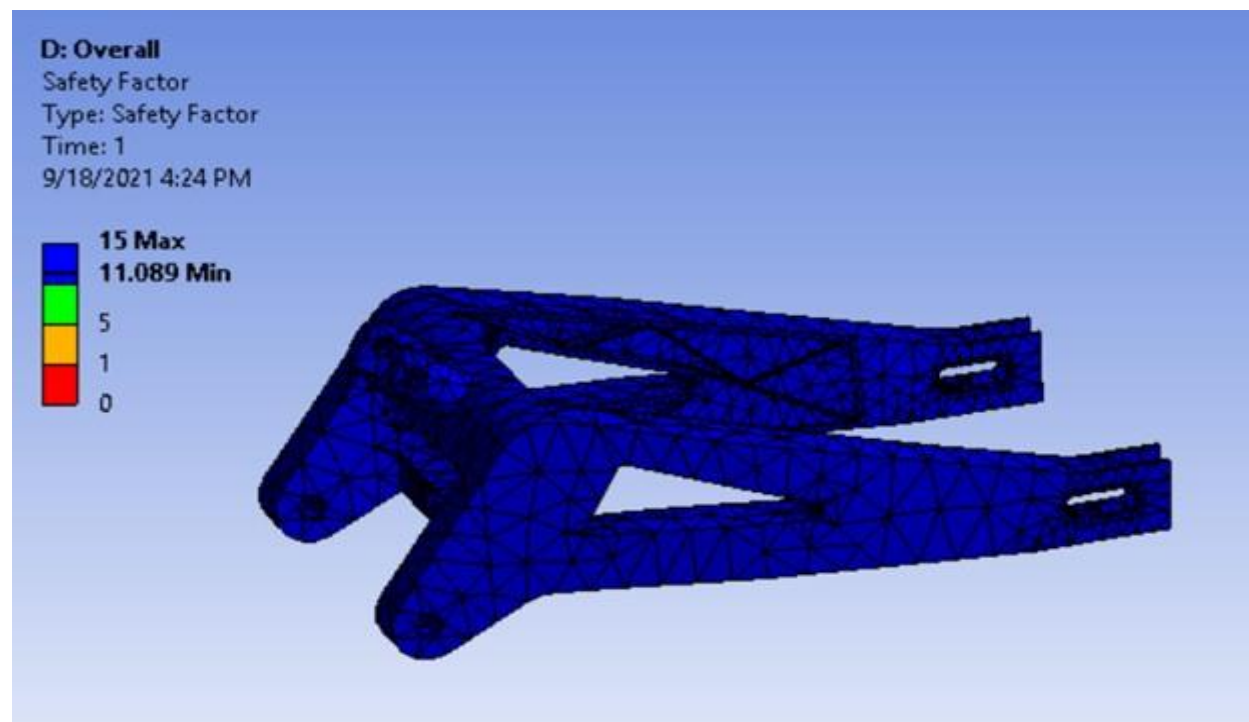
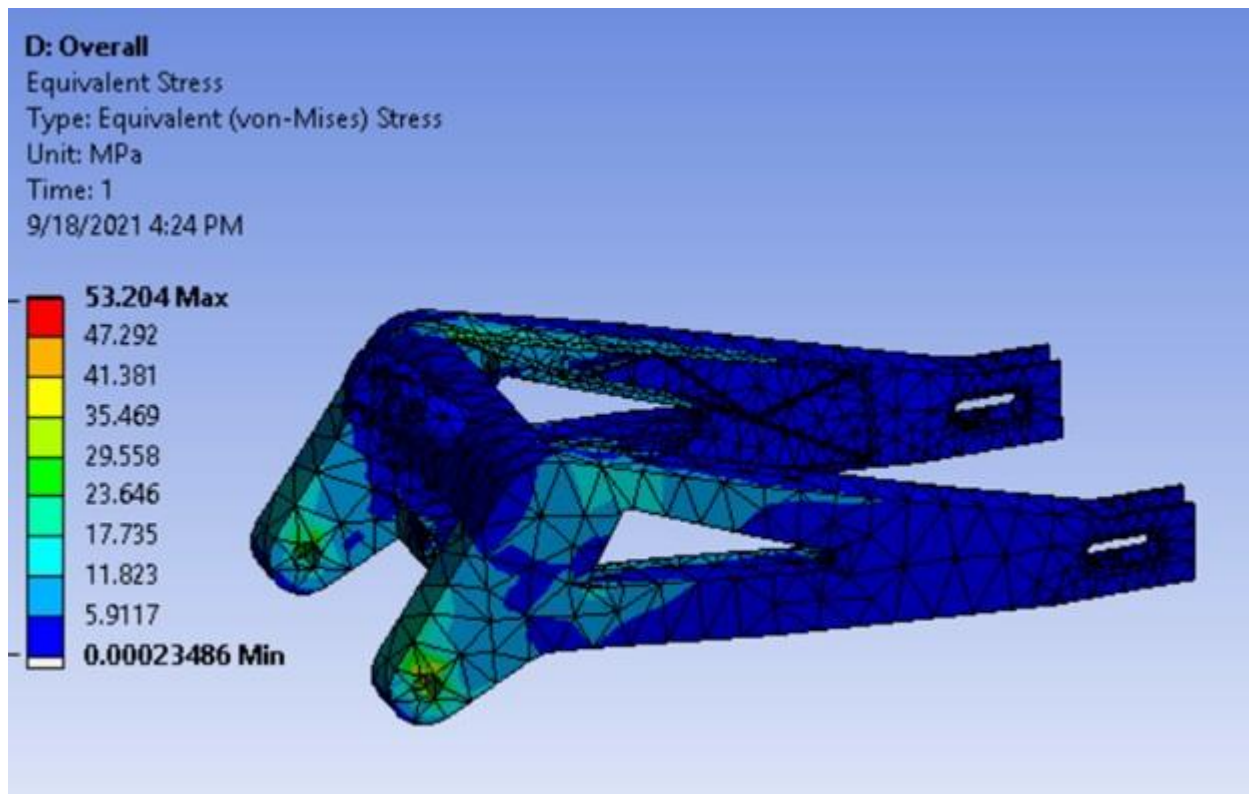


1. Overall : (Combined Forces)

[Type here]

S No.	Total Deformation (mm)	Von-Mises stress (Pa)	Factor of safety
1st Iteration	0.64022	67.71	15
2nd Iteration	0.61165	45.685	12.914
3rd Iteration	0.72792	53.204	11.089





	Mass (in kg)
1st Iteration	2.52
2nd Iteration	2.63
3rd Iteration	2.33

[Type here]

Observation:

After analyzing the different iterations of the swing arm while subjecting them to the same forces we can observe that the factor of safety of the swing arm decreases in all load cases while max deformation and equivalent stress almost remain similar. Even though the Von-Mises stress doesnot vary, the stress concentration is distributed more evenly throughout the swing arm thereby contributing to better fatigue life. The structural properties remain within allowable range while reducing the weight of the swing arm by 19 g . Weight savings is beneficial for the range of the vehicle as it reduces the resistive forces experienced by the vehicle while not having any negative structural impact.

We used Stress mappings and Topology optimization inorder to scrape out as much excessmaterial as possible without hindering much with the Factor of safety.

Modal analysis was performed and the swingarm was checked for its natural frequencies (modes) and the maximum deformation caused by each mode and in each direction. Having found out that the modes of our swingarm are well apart from the range of road frequencies stating that our swingarm was compatible and faced no excess deformation while just riding onroads.

Electrical System**1. Electrical vehicle model**

A model of the vehicle was created in Matlab Simulink to analyse the various parameters required for the battery pack. The parameters that we calculated are battery pack capacity and SOC for a required range. This is achieved by the following methodology:

Vehicle model

A physical model of the vehicle was created in Simulink. In order to calculate this multiple resistive forces like rolling force, aerodynamic force, gradient force and acceleration force is calculated using coefficient of rolling friction, gross vehicle mass, inclination of road surface, drag coefficient, frontal area, density of air and wheelradius as input parameters.

- I. $\text{Rolling force} = \text{Coefficient of rolling resistance} * 9.81 * \text{gross mass of vehicle}$
- II. $\text{Aerodynamic forces} = 0.5 * \text{density of air} * \text{frontal area} * \text{drag coefficient} * u^2$ Where u is vehicle velocity from drive cycle
- III. $\text{Gradient force} = 9.81 * \text{mass of vehicle} * \sin(\theta)$
Where θ is inclination angle of road surface
- IV. $\text{Acceleration force} = \text{mass of vehicle} * d^2u/dt^2$

1. Drive cycle data

Drive cycle source is provided to the vehicle model to determine the net power required to fulfill the cycle. FTP-75 (Federal test procedure) drive cycle data was utilized for providing drive cycle input to the vehicle model. Drive cycle source blockcontains velocity-time data for the vehicle.

2. Motor

Motor efficiency and gear ratio data is input to calculate power required to achieve desired torque to the rear wheel to overcome the resistive force on the rear wheel which is calculated from the above two sub-system.

3. Battery pack

After calculating the power requirement of the motor we calculate the battery capacity. Total number of cells in battery pack, no. of cells in series and parallel canbe calculated with cell capacity and battery back capacity. SOC is calculated using battery current discharged by the motor and the capacity of the battery pack.

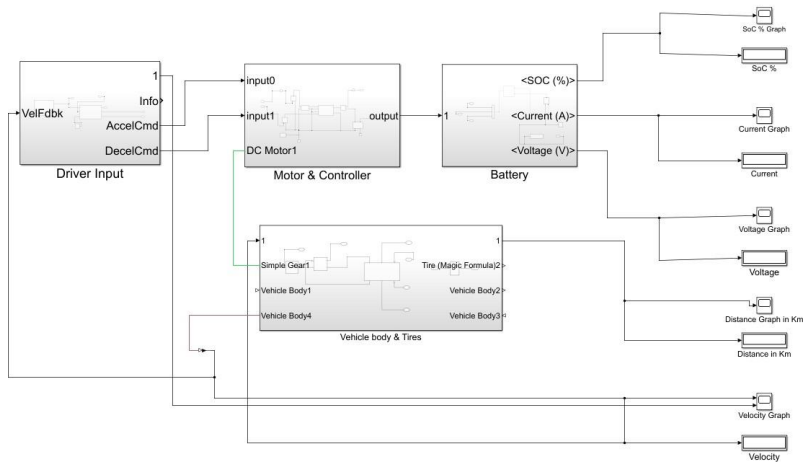


Fig: Simulink Model

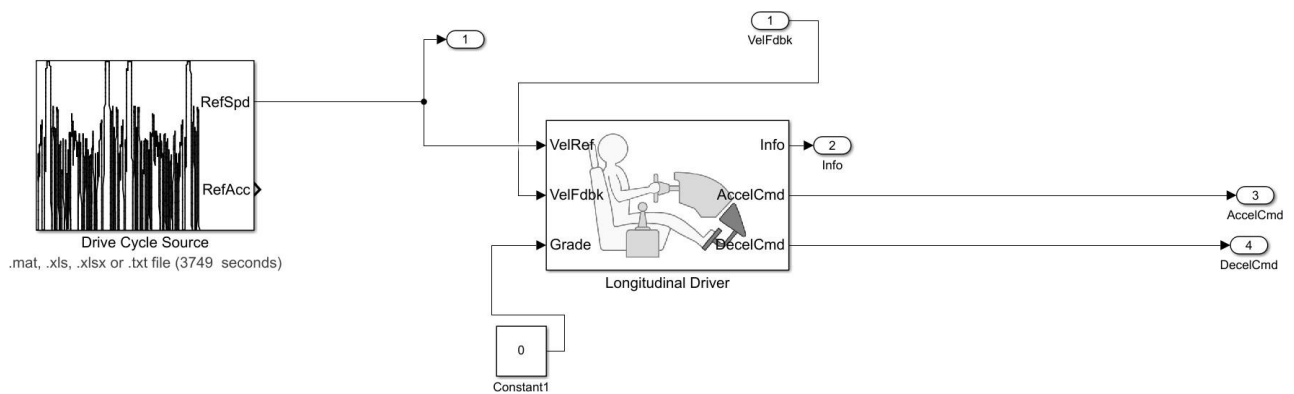


Fig: Driver Input Block

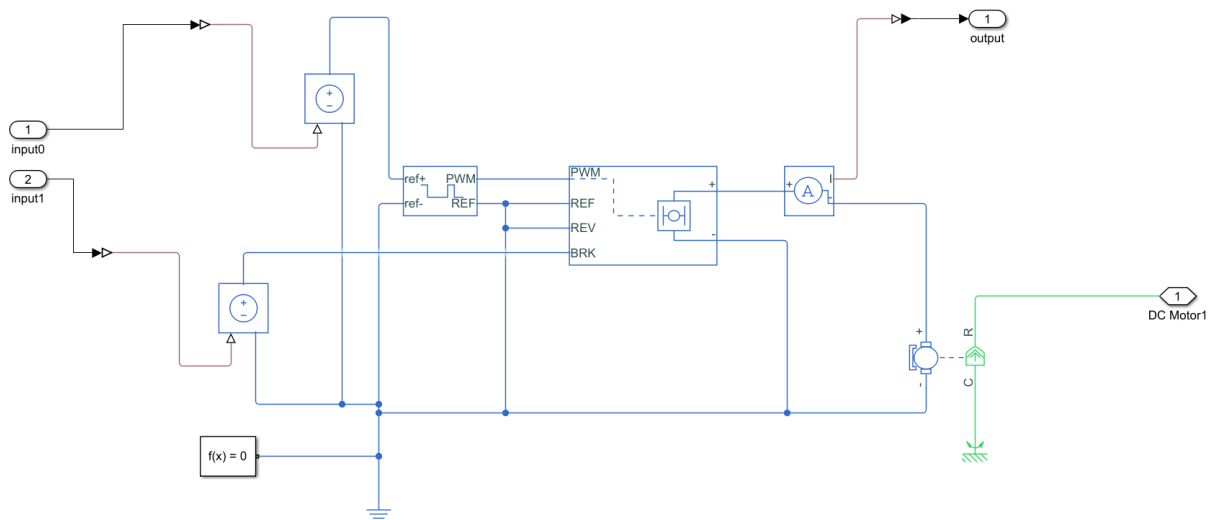


Fig: Motor and Controller Block

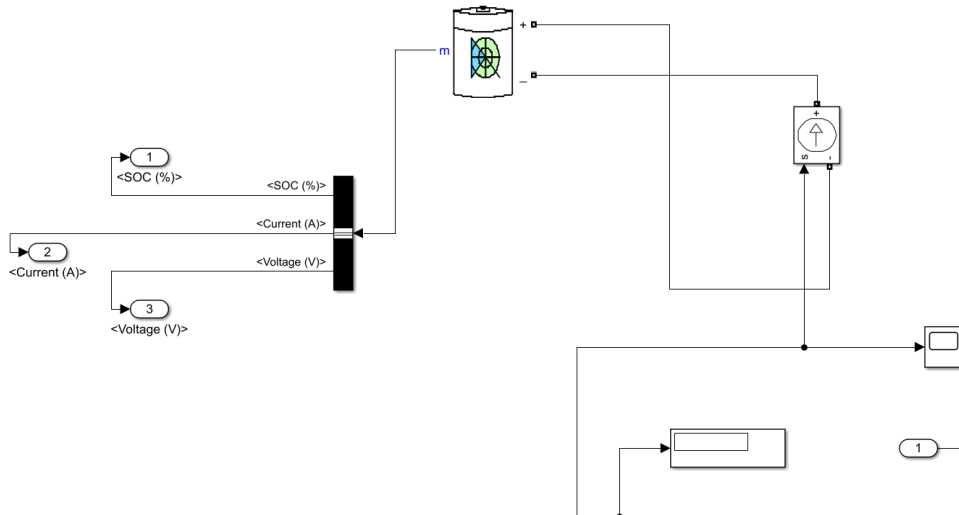


Fig: Battery Block

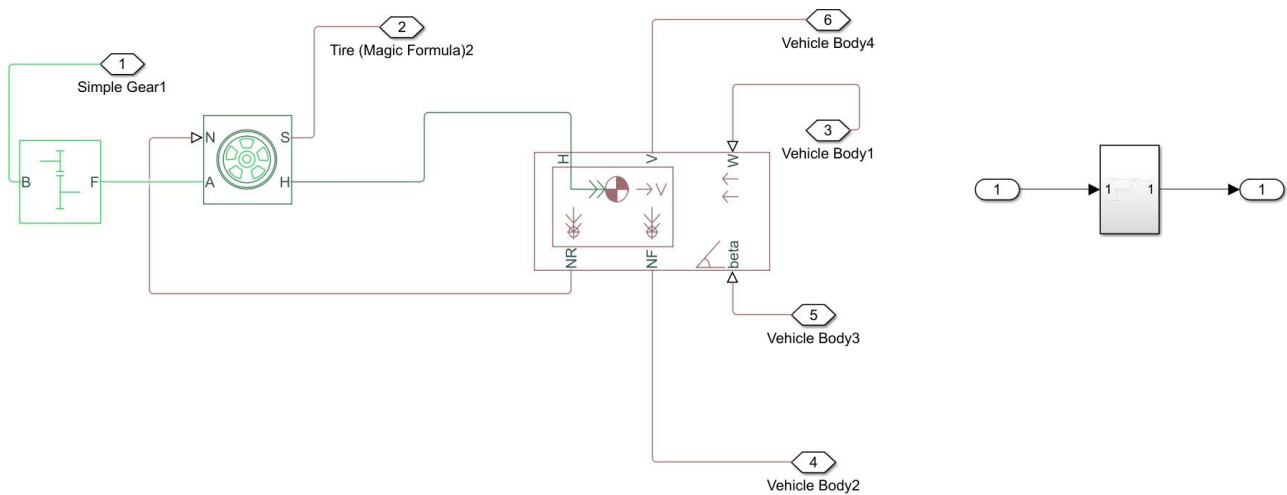


Fig: Vehicle Body and Tires Block

SOC was reduced from 100% to 10.5% after completing the drive cycle.

2. Cell : LG CHEM 18650 MJ1

Here we have chosen lithium ion cells over other cells due to following reasons:

1. High energy density
2. Low self-discharge
3. Low maintenance
4. Many options to choose in terms of capacity and geometry
5. Flexibility and high power to weight ratio
6. High life cycle

In cell selection we had many different types of cell chemistry and dimensions. So we did athorough research on which chemistry to choose among Lithium-Ion cells. The below tablegives the specification of the chosen cell.

CANBUS enabled controllers can be configured to take inputs from the battery management system and limit the amount of current the motor can draw.

1. Data Collection

The Orion Jr. 2 BMS collects data from several different sensors for use in calculations and decision making.

1.1. Cell Voltages - Each cell's voltage is measured approximately every 30 mS by sensing the voltage at the cell voltage tap connector. The BMS measures the difference in voltage from one tap wire to the next to measure a cell's voltage. Unless busbar compensation has been configured, the BMS will display and use the actual measured values for cell voltages (otherwise compensated values are used). Only the cell voltages which the BMS has been programmed to monitor in the cell population table in the settings profile are monitored while the other cell voltages are ignored.

1.2. Current (Amperage) - The current going in and out of the battery pack is measured every 8ms using the external hall effect sensor. The hall effect sensor is clamped around a wire carrying all current into and out of the battery pack and converts the measured amperage into two 0 - 5 volt analog voltages. One channel is used for measuring smaller amperages to ensure high resolution for small currents and the other channel is used for measuring larger currents. These two analog voltages are measured by the BMS and converted into an amperage value which the BMS uses for various calculations.

The current sensors sold with the Orion Jr. 2 BMS are available in sizes up to 1000A. The BMS can be configured to use 2 parallel current sensors to measure amperages up to 2000A, however the maximum recommended size is 1000A. Current sensors sold with the BMS are able to measure amperages up to 120% of their rated maximum, though accuracy is reduced above 100%. Current sensor data is used in calculating the battery pack's state of charge (via coulomb counting) and ensuring that the attached application is staying within the correct current limits. The measured current is also used in calculating the internal resistance and health of the cells in the battery pack.

1.3. Temperatures - The BMS measures battery temperatures directly from up to 3 thermistors to determine the average temperature of the battery pack. If additional temperature sensing, such as measuring the temperature of each individual cell, is required, the Orion Jr. 2 BMS can be connected to a thermistor expansion module which can allow measuring up to 80 thermistors. Thermistors on both the main unit and any expansion modules may be left 'unpopulated' meaning that the BMS will ignore the value of those thermistors. This allows the BMS to be configured to use as few or as many thermistors as necessary. The thermistor expansion module is connected to the Orion Jr. 2 BMS through two of the analog thermistor inputs on the BMS or via CANBUS if the BMS is CAN enabled.

1.4. Total Pack Voltage - The Orion Jr. 2 BMS measures the total pack voltage by summing up the individual cell voltages.

1.5. Other Inputs - The BMS has the ability to sense the status of the CHARGE power supply. The BMS uses this input to determine what mode the BMS is in. The BMS also has a multi-purpose input which can be used for various functions, including monitoring the status of the READY power source if necessary.

2. Thermal Management and Fan Control

The Orion Jr. 2 BMS measures the battery temperature through 3 main thermistors connected directly to the BMS with the option of additional thermistors through a thermistor expansion module. The BMS calculates the minimum, maximum, and average temperatures of the battery pack based on the attached thermistors. These temperature readings are used in the calculation of maximum possible charge and discharge current limits, which are used to determine when and at what amperage a battery pack can be charged or discharged. The multi-purpose outputs may be programmed to turn on or off at specific temperatures, which may be useful in some applications.

3. Cell Balancing

The BMS takes an intelligent approach to balancing that seeks to maintain and improve balance from cycle to cycle. Li-ion batteries tend to stay in balance unlike the lead acid ones. Differences in self discharge rates, cell temperature and internal resistance are the primary causes of an unbalanced battery pack. The BMS must be able to add or subtract charge from the lowest or highest cells to compensate for the difference in discharge rates to keep the cells balanced.

The Orion Jr. BMS uses passive balancing to remove charge from the highest cells in order to maintain the balance of

[Type here]

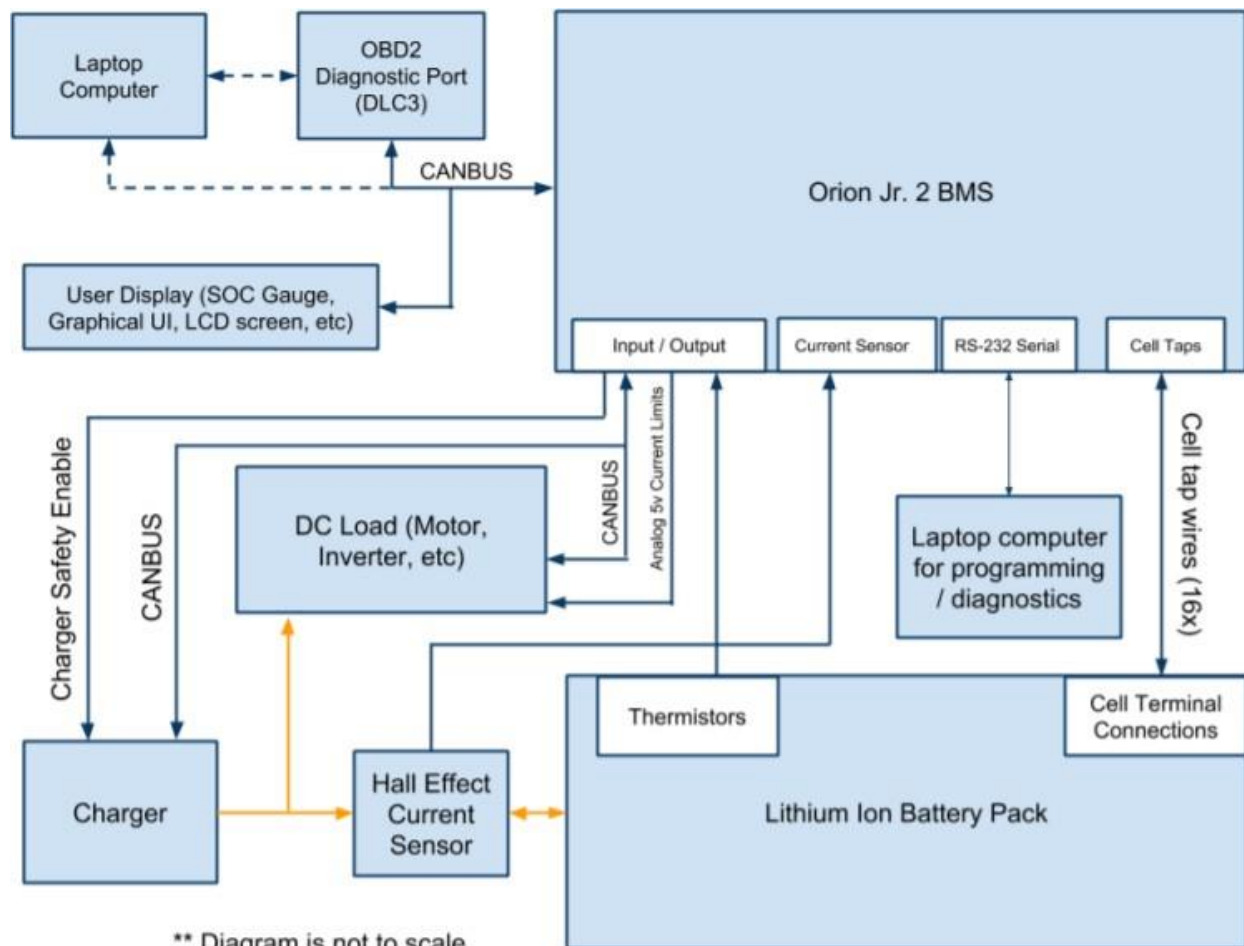
the pack using passive shunt resistors.

The BMS has a safety feature to prevent over-discharging any cell during balancing in the event of a defective or dead cell

4. CANBUS

The Orion Jr. BMS has an optional CAN (controller area network) interface. The interface has a programmable frequency (baud-rate). The BMS features up to 15 programmable CAN. These messages are designed to be flexible to interface with other electronic control units, computer systems, displays, or any number of different devices. Virtually all BMS parameters are able to be transmitted in these CAN messages. Please see the "Editing CAN Messages" section of the Software Utility manual for details on programming custom CAN messages. In a CANBUS network there are always exactly two terminator resistors. It is up to the user to ensure that there is the proper number of terminator resistors on each CAN network. By default, the Orion Jr. BMS has a terminator resistor already loaded on the CAN interface. The CAN interface may also be used to upload settings. However, all BMS firmware updates must be performed using the RS-232 serial interface. Firmware updates may be necessary to add additional future functionality.

Cell Broadcast Option - The BMS can be configured to rapidly transmit cell voltages onto the CANBUS. This is useful when data logging as it is the fastest method for the BMS to transmit cell voltages

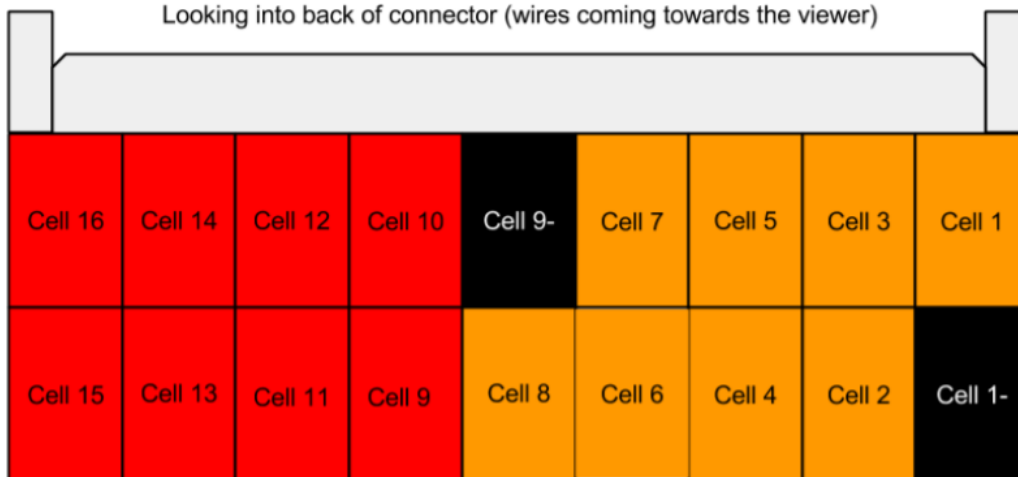




Connector locations on the Orion Jr 2. BMS as looking at the BMS from the top

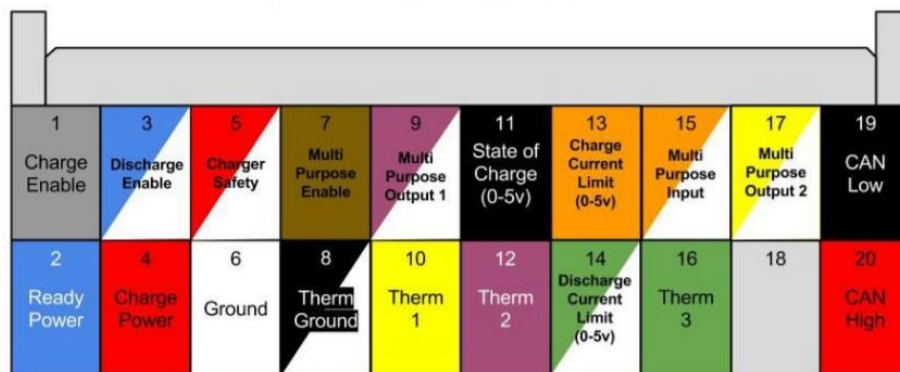
Cell Tap Wiring Diagram

Looking into back of connector (wires coming towards the viewer)



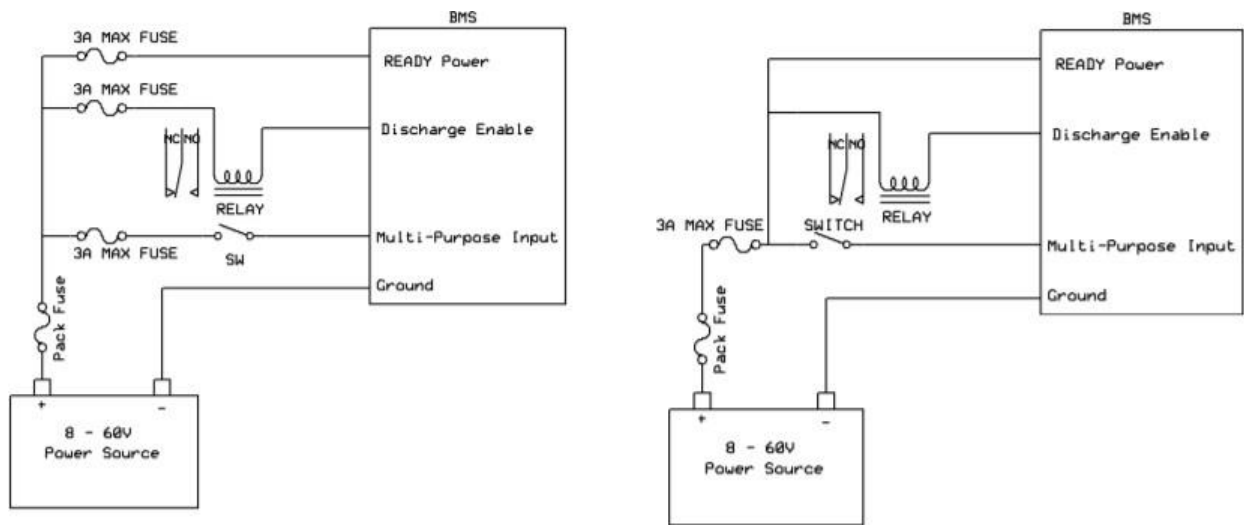
Looking into back of connector (wires coming towards the viewer)

Main Input/Output (I/O) Connector



Looking into back of connector (wires coming toward viewer)

5. Fuse Placement



6. Motor: ATO 2kW, 48V BLDC Motor

1. MOTOR SELECTION: For our prototype, we have chosen to use a permanent magnet motor. Permanent magnet motor used here is the Brushless DC motor. We have chosen this machine due to its three major advantages:

1.1. High Efficiency:

The PM machines have very high efficiency as they use PM (Permanent magnets) for the excitation of the motor, without consuming any power. And there are no mechanical commutators and carbon brushes which reduce the mechanical friction losses.

1.2. High power density:

The use of high energy dense magnets made from rare earth magnets allowed us to achieve very high flux density in the PM machines. Due to high flux density, high torque can be achieved and this has considerably reduced the size and made it more compact.

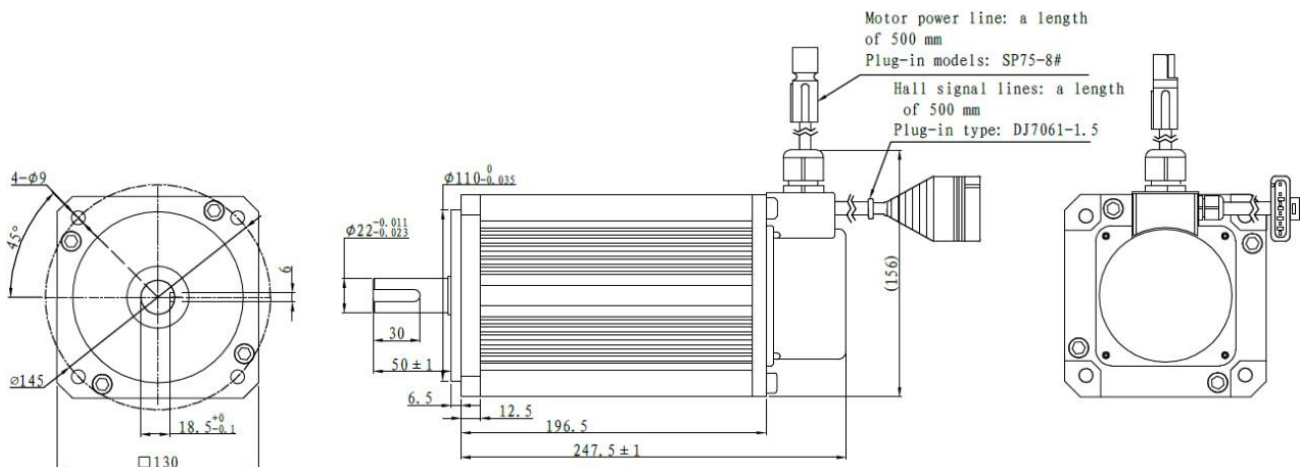
1.3. Ease of control:

They can be easily controlled just like DC machines due to easy access to the control variables and consistency in their output

2. MOTOR SPECIFICATION:

Parameter	Rating
Rated Power	2kW
Rated Torque	10Nm
Peak Torque	30Nm
Operating Voltage	48V
Rated Current	51.3A
Rated RPM	2000
Maximum RPM	2400

3. DIMENSIONAL SPECIFICATION:



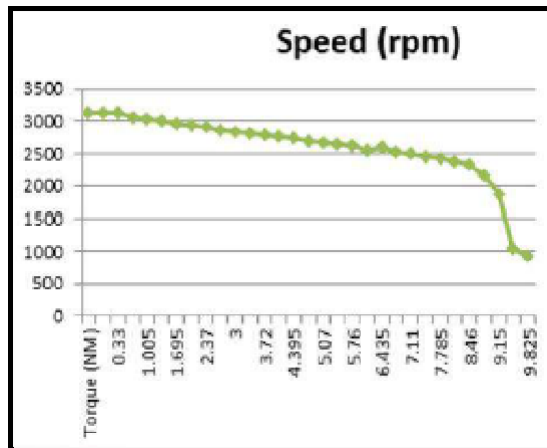
4. KEY FEATURES:

- 4.1. High efficiency and high torque
- 4.2. Low noise operation due to absence of brushes
- 4.3. High power to weight ratio
- 4.4. Smaller and compact geometry
- 4.5. Forced air cooling for higher heat dissipation
- 4.6. Optimal current consumption
- 4.7. Low hysteresis loss material used (Silicon steel)
- 4.8. High power Neodymium Magnet
- 4.9. High quality heavy duty multi-stranded (53 strand) wire used
- 4.10. High temperature resistant coated wires used
- 4.11. No lubrication required
- 4.12. High speed of operation even in loaded and unloaded conditions due to the absence of brushes that limits the speed

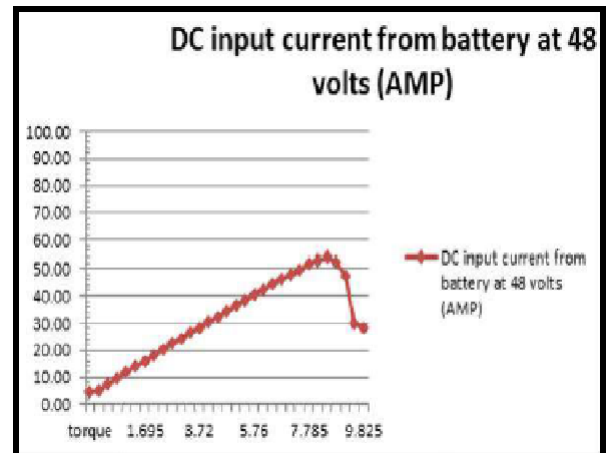
[Type here]

5. MOTOR CHARACTERISTICS:

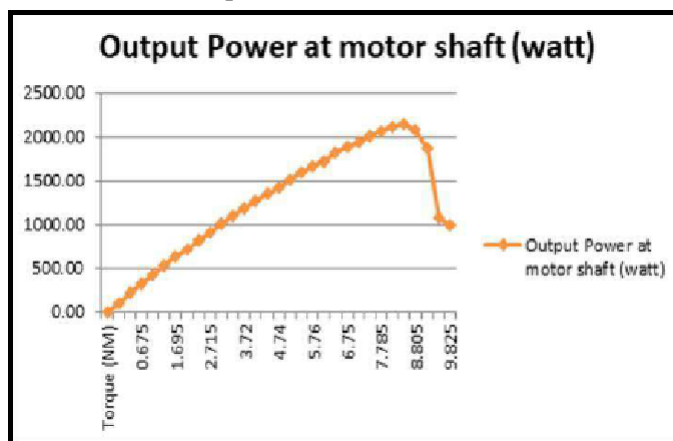
Torque vs RPM:



Torque vs Voltage:



Torque vs RPM:



Torque (NM)	Speed (rpm)	DC input current from battery at 48 volts (AMP)	output Power at motor shaft (watt)	efficiency %
0	3135	4.50	0.00	0.00
0.33	3123	5.40	107.89	41.28
0.675	3126	7.60	220.88	60.51
1.005	3062	9.79	322.08	68.50
1.35	3030	11.86	428.21	75.19
1.695	2997	14.16	531.74	78.23
2.025	2965	16.12	628.42	81.19
2.37	2934	18.36	727.71	82.57
2.715	2903	20.37	825.00	84.38
3	2871	22.45	901.46	83.64
3.375	2842	24.40	1004.08	85.66
3.72	2813	26.61	1095.25	85.75
4.065	2786	28.46	1185.51	86.80
4.395	2760	30.38	1269.08	87.04
4.74	2730	32.40	1355.03	87.13
5.07	2700	34.52	1433.23	86.51
5.415	2670	36.44	1515.15	86.63
5.76	2645	38.40	1593.92	86.48
6.09	2615	40.34	1666.47	86.07
6.435	2560	42.26	1724.41	85.02
6.75	2590	44.22	1828.95	86.17
7.11	2535	46.07	1885.49	85.27
7.455	2500	47.94	1950.30	84.75
7.785	2460	49.73	2005.66	84.03
8.13	2430	51.54	2066.25	83.52
8.46	2390	52.95	2117.32	83.31
8.805	2336	54.14	2152.88	82.85
9.15	2166	52.28	2074.38	82.67
9.495	1876	47.49	1864.64	81.80
9.825	1050	29.91	1080.49	75.26
10.17	938	28.23	998.09	73.66

7. Motor Controller: ATO Motor Controller

Motor controller serves to govern in a predetermined manner the performance of the motor. It includes hall sensor, govern the amount of current by motor, selecting and regulating the speed, selecting forward and reverse rotation, regulation of current and potential, and protecting against overloads and faults.

ATOTH-G series programmable controller is dedicated to an efficient, stable and easy to install electric vehicle controller design, suitable for electric bicycles, electric motorcycles and electric scooters etc.. The series controller is able to output a high starting current and supply a tight battery current limit. Therefore, it can work in relatively small battery current conditions, and can provide a good acceleration and climbing ability.

ATOTH-G controller uses high power MOSFET high frequency design, the efficiency is upto 99%. An intelligent microprocessor provides a comprehensive and accurate control for the ATOTH-G controller.

[Type here]

7.1. Features:

- 7.1.1. Designed for electric motorcycles and electric scooters.
- 7.1.2. Powerful and intelligent microprocessor.
- 7.1.3. High-speed low-loss synchronous rectification PWM modulation.
- 7.1.4. Strict current limit and torque control.
- 7.1.5. Limiting the battery current function will not trigger the battery current limit protection and extend battery life.
- 7.1.6. Greater starting current can get a faster start-up speed.
- 7.1.7. Anti-electromagnetic interference and anti-vibration performance.
- 7.1.8. Fault indicator indicates a variety of failures for user-friendly testing and maintenance.
- 7.1.9. With electronic switching function.
- 7.1.10. It has a battery protection function: When the battery voltage is low, the alarm will be timely and the current attenuation, low output to stop the protection of the battery.
- 7.1.11. Beautiful and fast heat dissipation of aluminum with a heat spur shell.
- 7.1.12. With over-temperature protection: when the temperature is too high or too low will automatically current attenuation to protect the controller and battery.
- 7.1.13. Compatible with 60 degrees or 120 degrees Hall position sensor.
- 7.1.14. Support any poles of brushless motor.
- 7.1.15. Up to 40000 electric RPM. (electric RPM = mechanical speed * motor pole pairs).
- 7.1.16. The brake switch is used to control the regenerative braking.
- 7.1.17. 0-5V brake signal is used to control regenerative braking.
- 7.1.18. High pedal protection: The pedal signal is detected when the key is turned on, and is not output if a valid signal is present.
- 7.1.19. Three power generation modes: brake switch power generation, release pedal power generation and 0-5V analog signal power generation.
- 7.1.20. Current multiplication: Small battery current can get larger motor output current.
- 7.1.21. Easy to install: use a 3-wire pedal potentiometer to work.

7.2. Basic Functions:

- 7.2.1. Fault detection and protection. It can identify faults via LED twinkling code.
- 7.2.2. Battery voltage real-time monitoring. It will stop working when the battery voltage is higher or lower.
- 7.2.3. Built in current detection and over current protection.
- 7.2.4. The controller is equipped with temperature measurement and protection functions. At low and high temperatures, the current is cut to protect the controller and the battery. If the controller temperature is higher than 90°C, the current will be a sharp decline. It will automatically cut off the output when it up to 100°C. At low temperatures, the current typically begins to drop at 0 °C.
- 7.2.5. At power-up, the voltage is constantly monitored by the controller. If it is found that the voltage is too high, the controller will immediately cut the current until the power generation stops.
- 7.2.6. The maximum speed can be configured half the maximum forward speed.
- 7.2.7. 5V sensor power supply.
- 7.2.8. 3 switch inputs. Connect to GND for a valid signal. The default is the pedal safety switch input (to be configured via the customer software), the brake switch input and the reversing switch input.
- 7.2.9. Three 0-5V analog inputs. The default is the pedal analog signal input, the brake analog signal input and the motor temperature sensor analog signal input.

[Type here]

- 7.3. Specifications:
- 7.3.1. Working frequency: 16.6KHz
- 7.3.2. Standby current: Less than 0.5A
- 7.3.3. 5V sensor supply current: 40mA
- 7.3.4. Supply voltage: 72V and 18V~72V
- 7.3.5. Supply current: 150mA
- 7.3.6. Working voltage: 18V to 1.25* nominal value
- 7.3.7. Standard throttle input: 0-5V (Three wire resistance type), 1-4V (HALL type)
- 7.3.8. Brake analog signal and throttle signal input: 0-5V. Using three wire resistance type pedal to produce 0-5V signal
- 7.3.9. Full power operating temperature range: 0°C~50°C(Controller shell temperature)
- 7.3.10. Working temperature range: -30°C-90°C, 100 °Cshutdown (Controller shell temperature)
- 7.3.11. Peak phase current, 10s: 50-120A (According to the model)
- 7.3.12. Continuous phase current: 5-50A (According to the model)
- 7.3.13. Maximum battery current: adjustable (Note: The default maximum current is set to 70%)
- 7.3.14. The input current of the controller shall be 1.5 times the rated current of the motor.

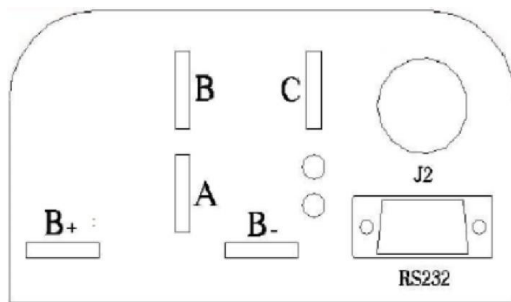


Figure : Brushless motor controller front panel

B⁺: Battery positive

B⁻: Battery negative

A: Output U/1/A phase, connect motor with thick yellow line

B: Output V/2/B phase, connect motor with thick green line

C: Output W/3/C phase, connect motor with thick blue line

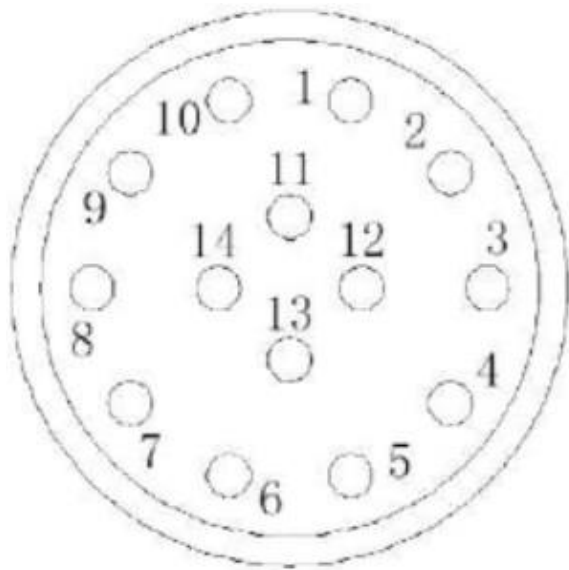


Figure : J2 pin position

1. PWR: Controller power supply (input)
2. RTN: Signal return, or power supply return
3. RTN: Signal return
4. 12V high-level brake and motor temperature input
5. Throttle analog input, 0-5V
6. Brake analog input, 0-5V
7. 5V: 5V supply output, <40mA
8. Throttle switch input
9. Reversing switch input
10. Brake switch input
11. Hall phase C
12. Hall phase B
13. Hall phase A
14. RTN: Signal return

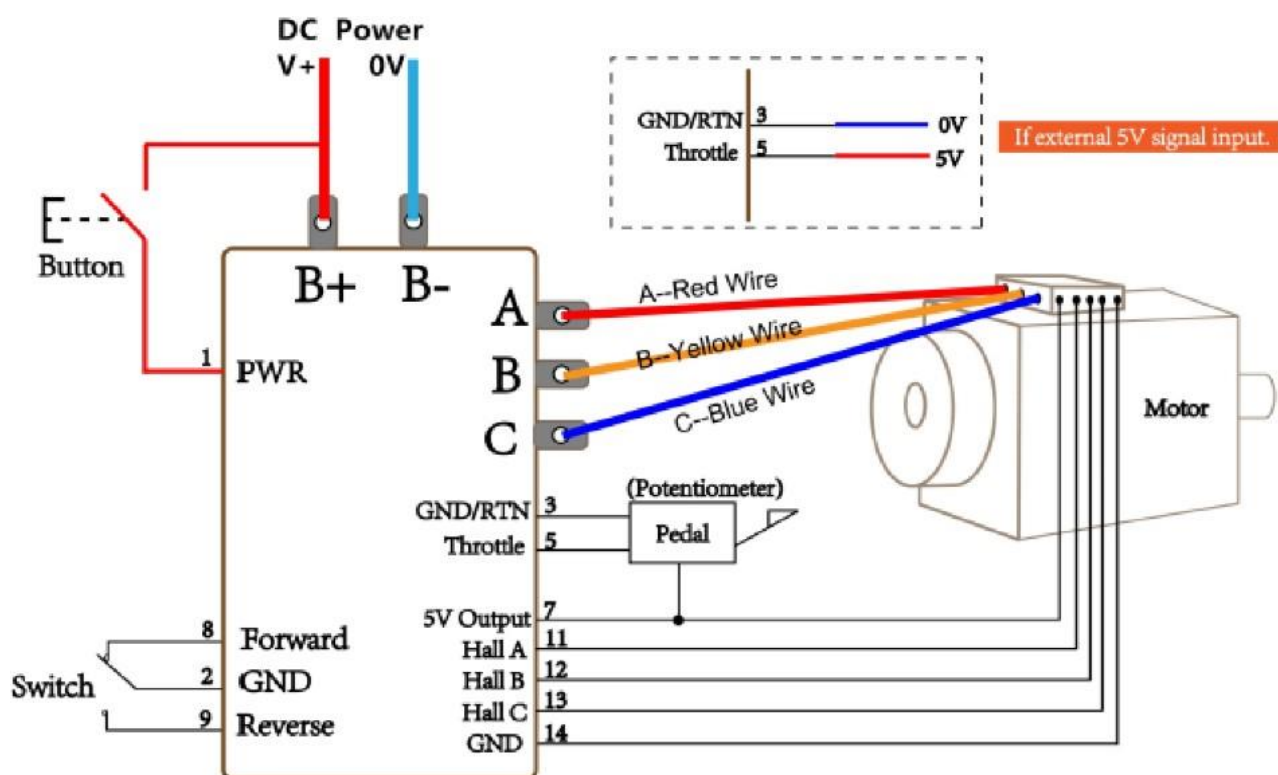
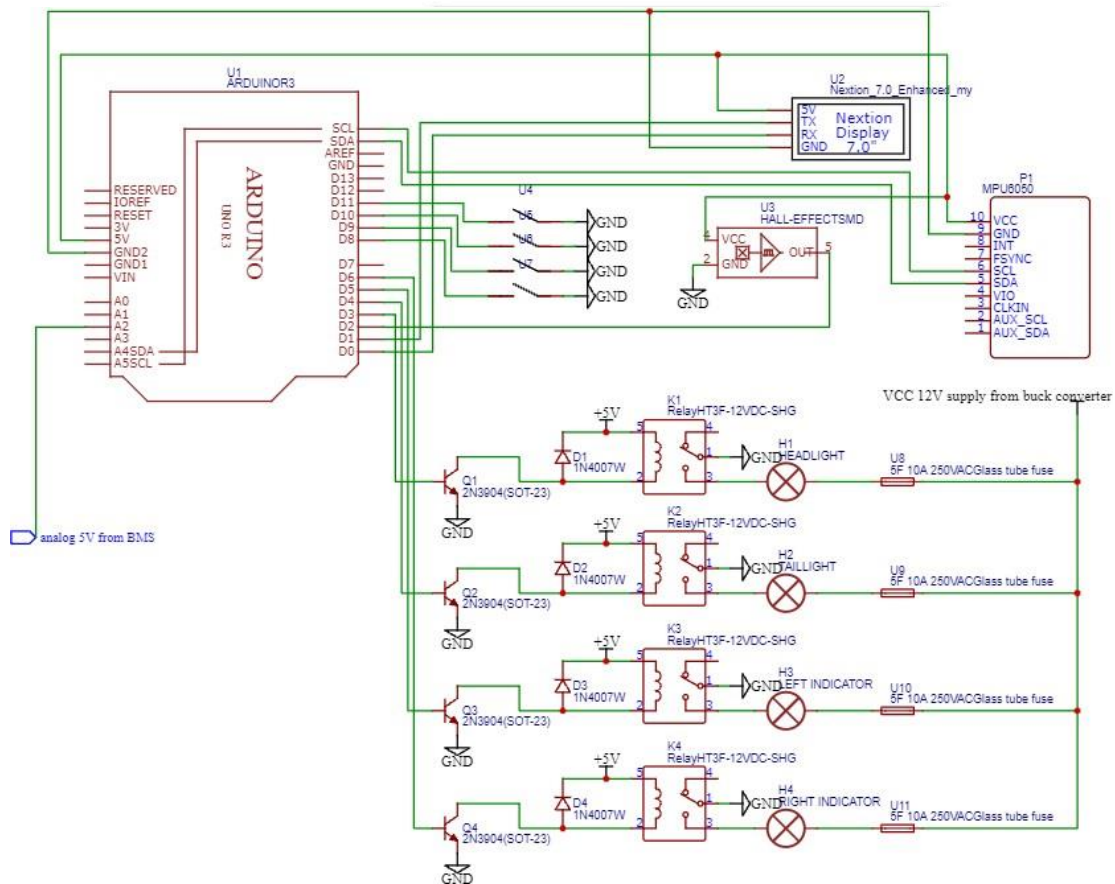


Figure : TH-G controller standard wiring

7.4. Communication Port:

A RS232 port is provided to communicate with host computer for calibration and configuration.

[Type here]



A. Microcontroller

8. Low Voltage System

Arduino Uno is a

microcontroller board based on the ATmega328P (datasheet). It has 14 digital input/output pins (of which 6 can be used as PWM outputs), 6 analog inputs, a 16 MHz ceramic resonator (CSTCE16M0V53-R0), a USB connection, a power jack, an ICSP header and a reset button. It contains everything needed to support the microcontroller; simply connect it to a computer with a USB cable or power it with a AC-to-DC adapter or battery to get started.

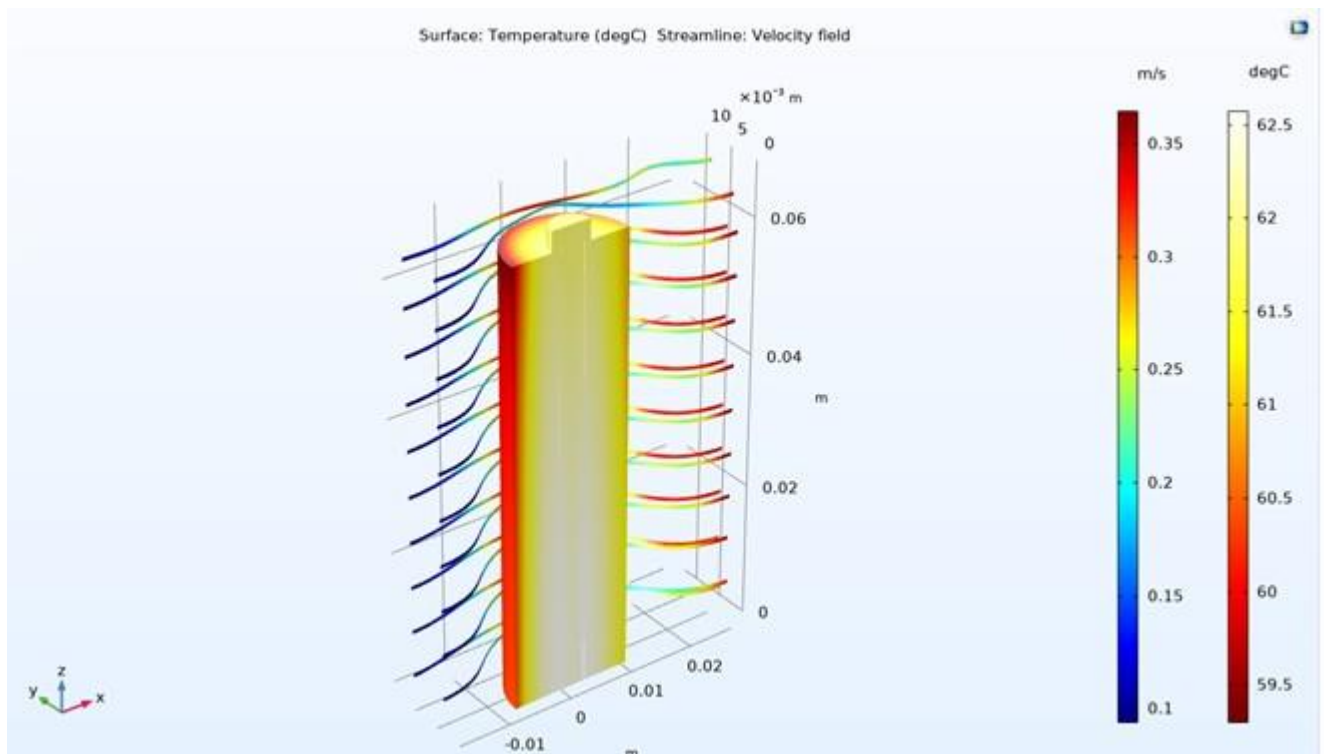
Thermal Simulation

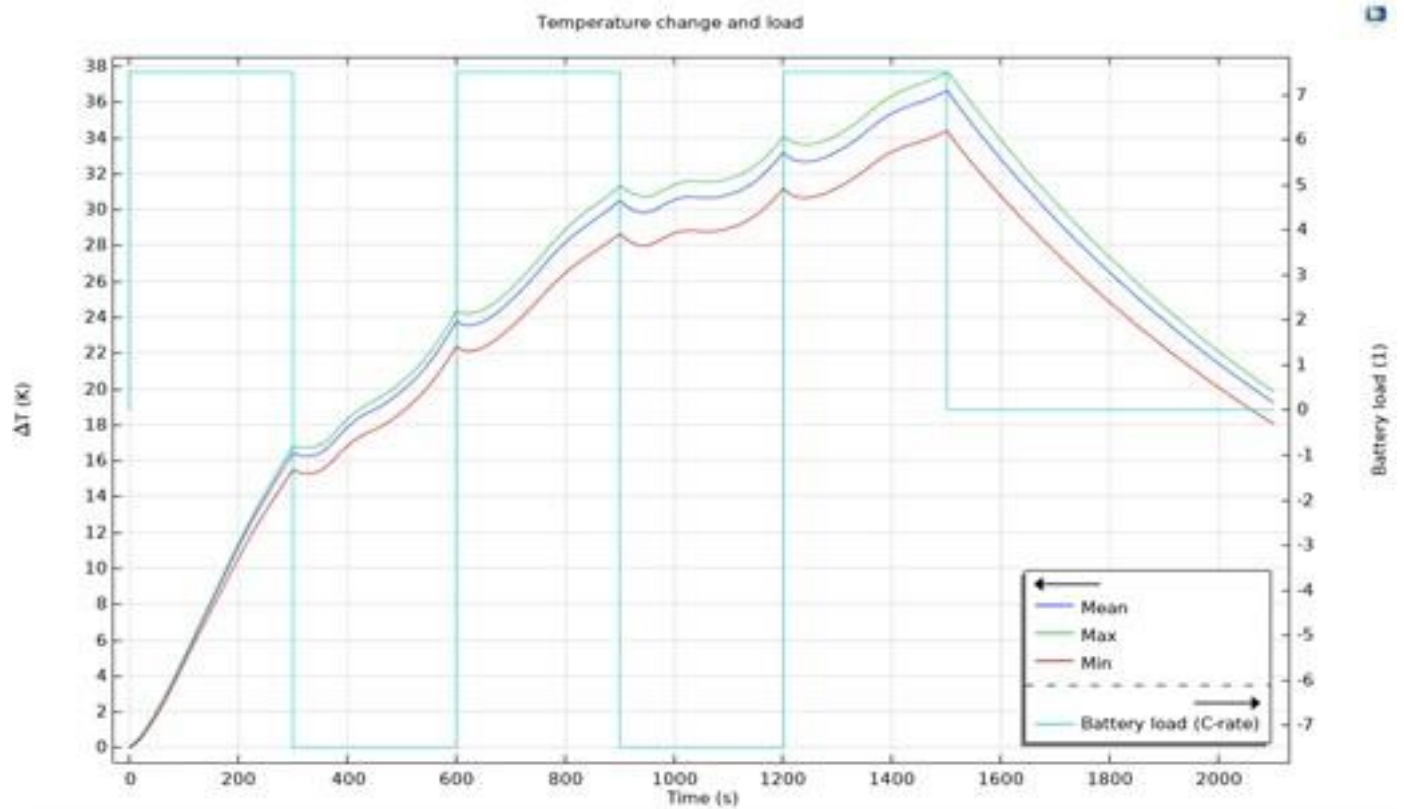
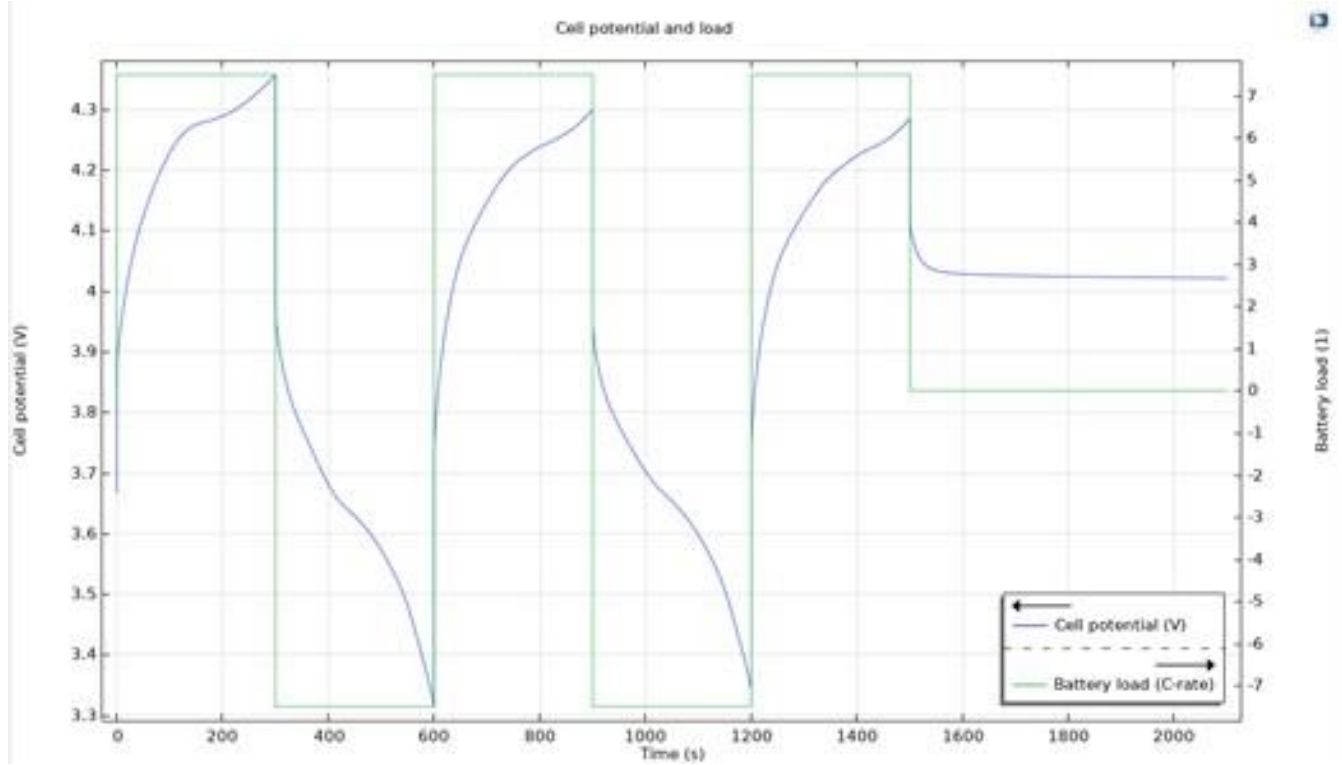
The main heat dissipation components are battery and motor. Heat transfer between battery modules occurs via three different processes. Convection, Black body radiation and conduction. The amount of heat transfer through radiation is nearly negligible when compared to the other modes. So, the main heat process in our system is via convection and conduction.

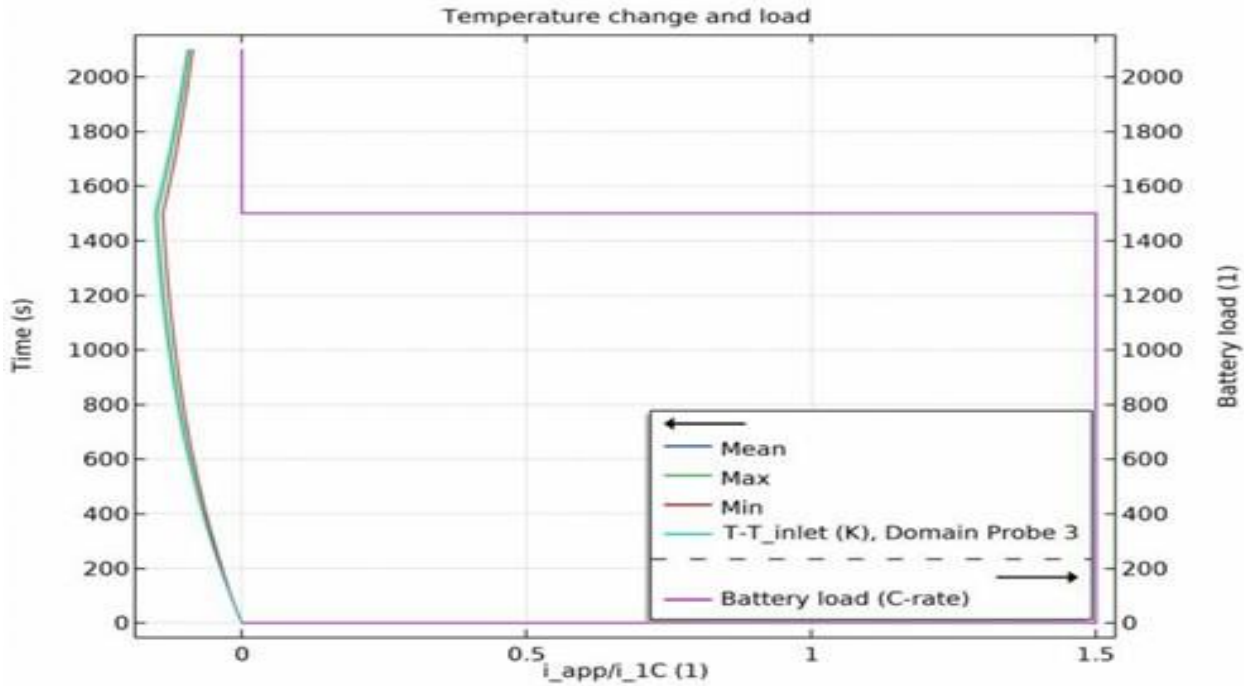
The thermal distribution analysis has been performed in COMSOL Multiphysics. High temperature generation regions have been identified and represented in the following section to understand the thermal behavior of the battery pack.

1. Thermal Distribution of a cell

Individual cell behavior was studied and the results obtained have been presented below:

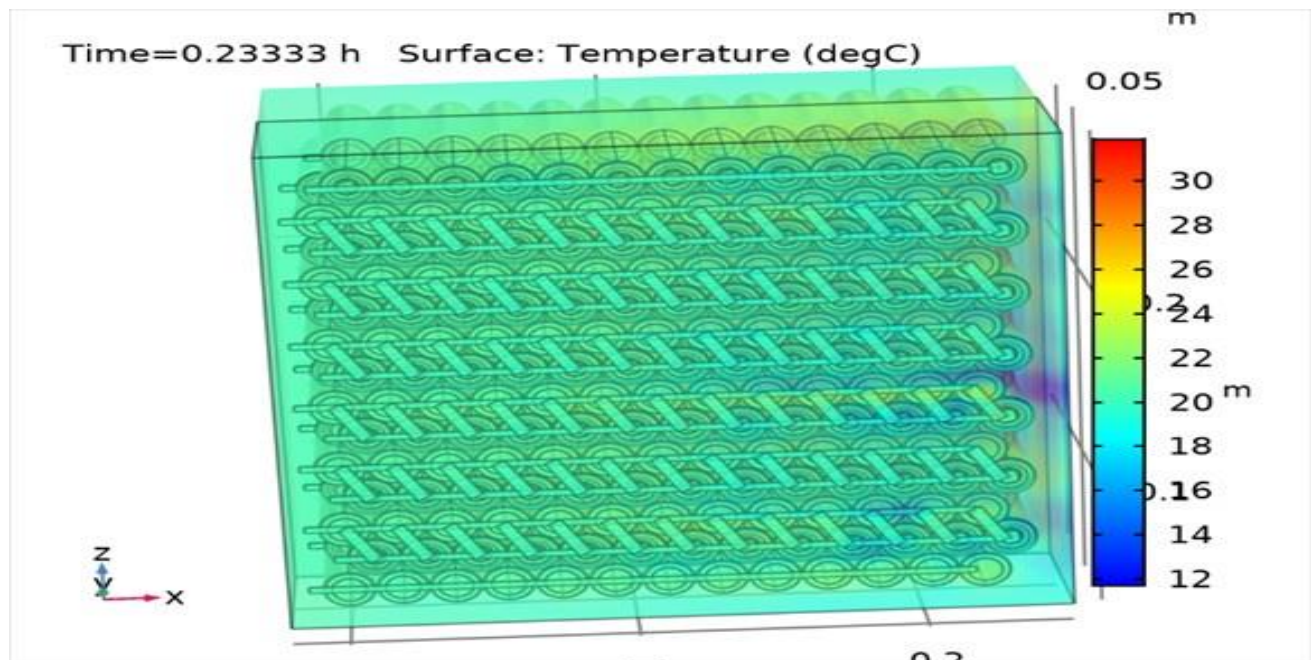






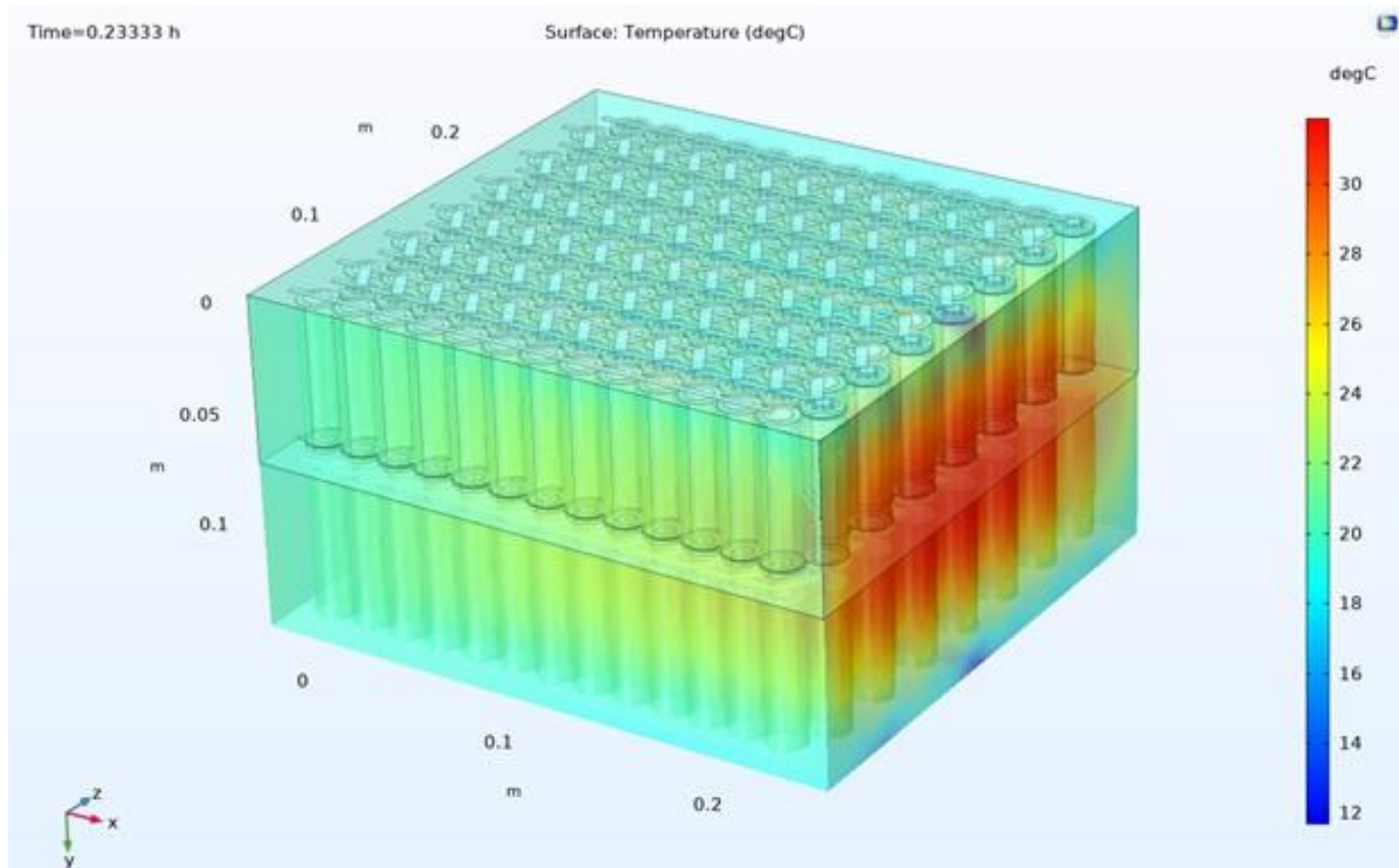
The Thermal analysis shows the temperature in the battery and streamlines for the flow at 1600s to 7000s respectively. The maximum temperature is located in the active battery material towards the thermally isolated end.

2. Thermal Distribution of battery(pack) accumulator



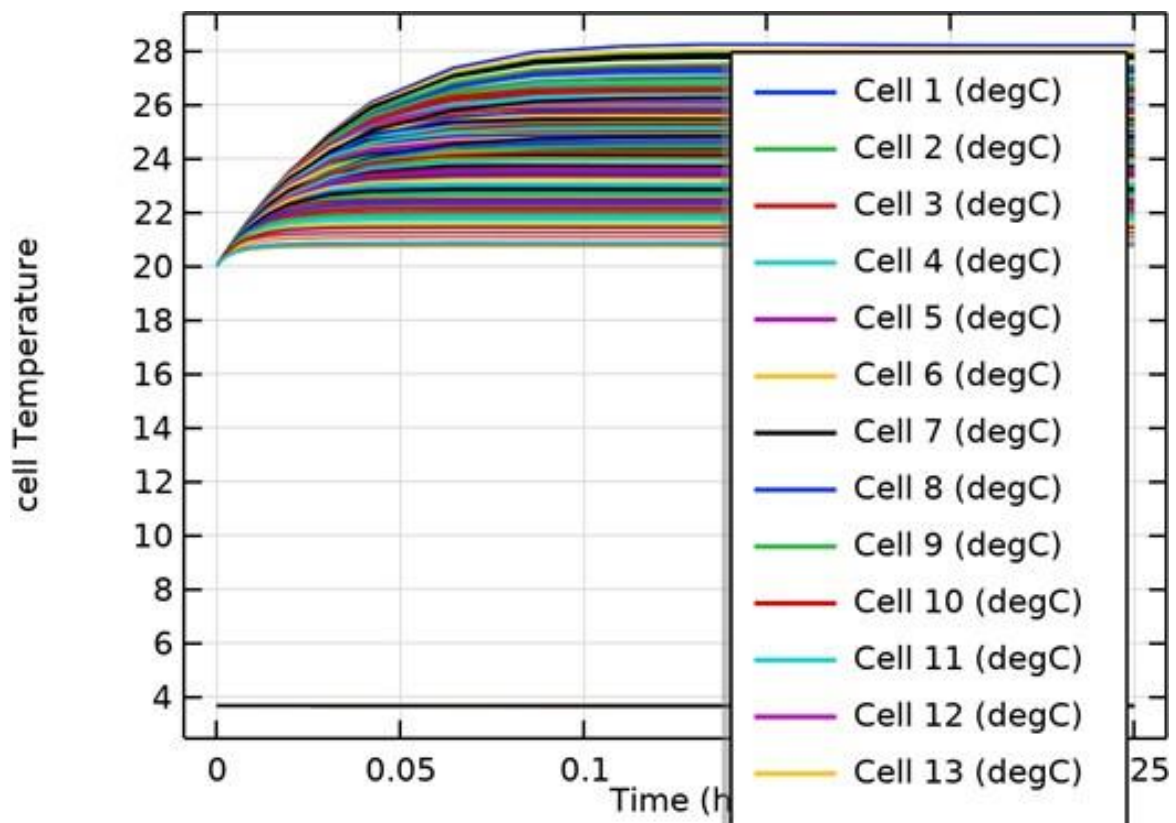
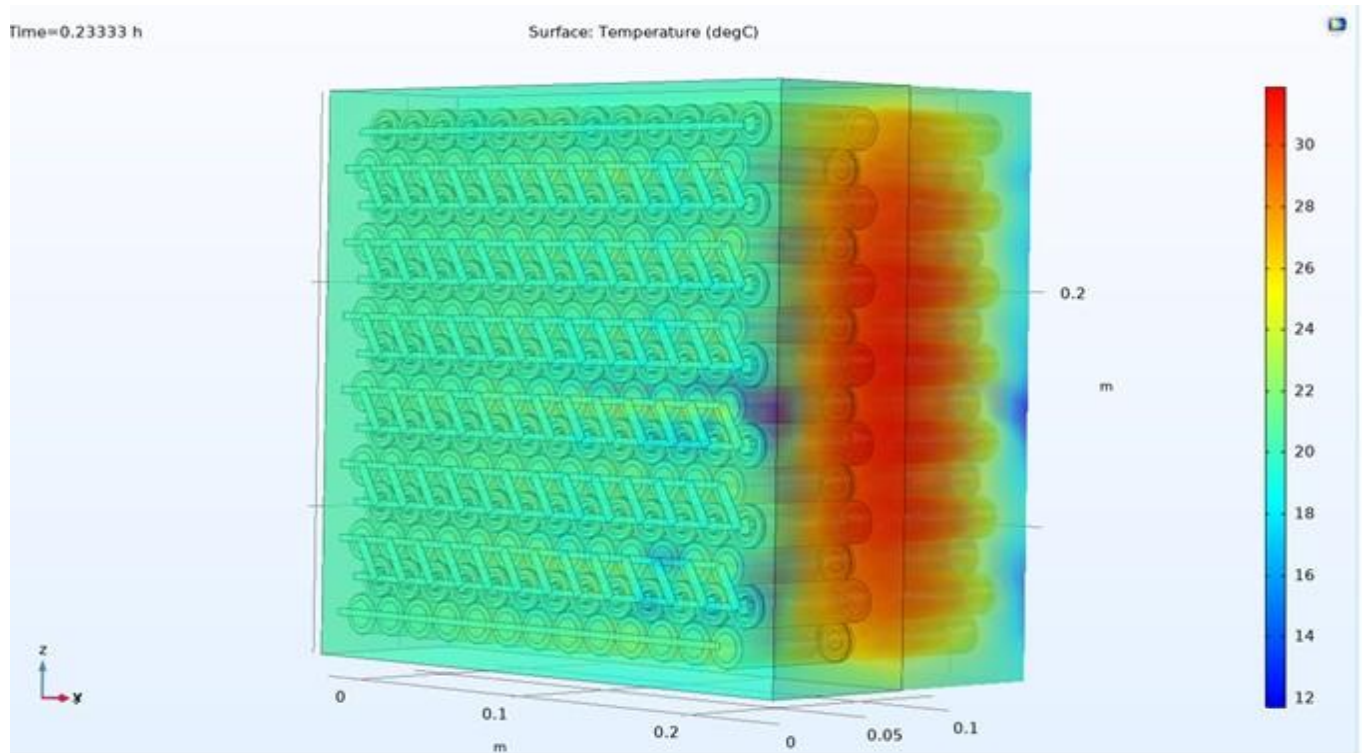
Battery accumulator behavior was studied, and the results thus obtained, have been presented below:

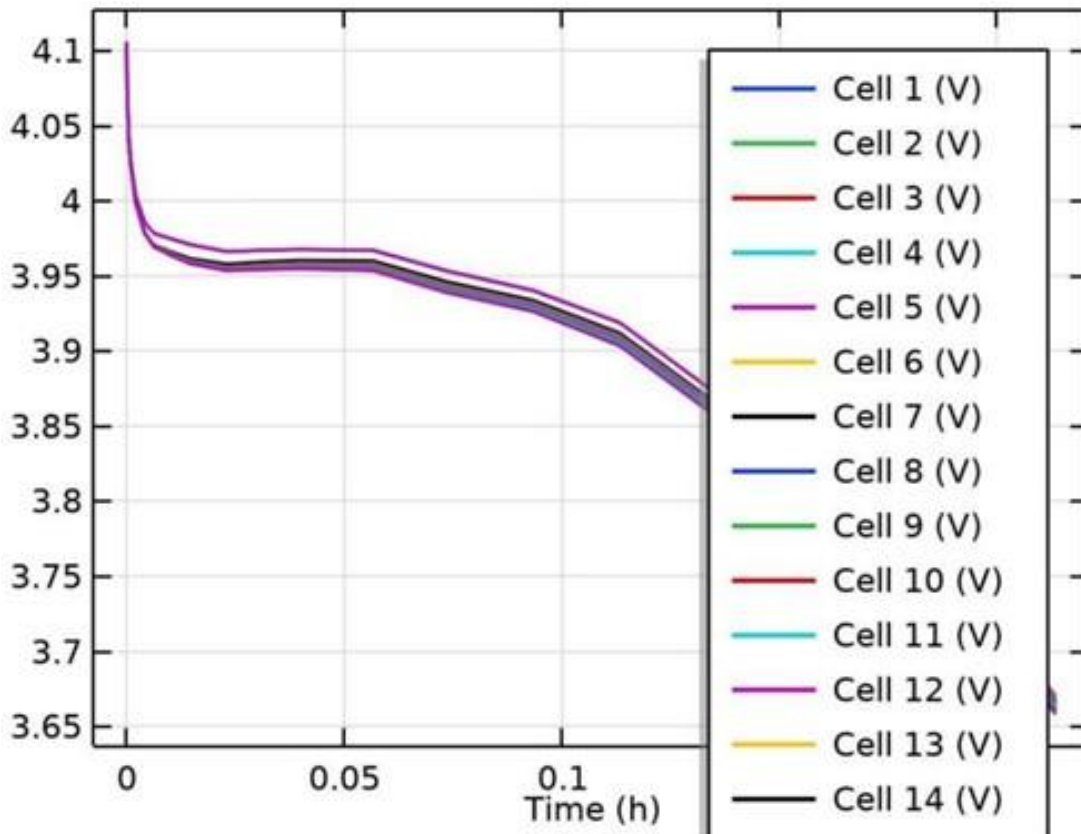
[Type here]



The thermal analysis shows the surface temperature in the battery accumulator at 720 s(0.2 h). We have allowed natural air flow with velocity as 11 m/s in x direction .

Faces perpendicular to the z-axis are insulated. Maximum temperature reached by the accumulator in the given stimulation is 34°C .





Powertrain

Transmission System

The transmission of a bike is one of the most important systems responsible for transmitting power from the propeller to the wheels. The components need to be highly reliable under all situations and strong enough to withstand any stresses they may face. Having established this, the chain is designed to be the weakest member of the system as it is cheaper and easily replaceable. The transmission system consists of a duplex chain to transmit power from the motor to a reducer box. The reducer box is made of helical gears submerged in oil contained in a metallic shell. The power further is transmitted to wheels using a chain.

Constant Reduction

1. If a constant gearbox reduction is not used, the size and weight of the sprocket will be very large, almost the size of a rim, because of such weight the centre of mass of the vehicle will shift backwards.
2. Increase the torque and speed will also be optimized to give better performance.
3. If the chain of the final drive is not the weakest member then it will affect the motor or else the motor shaft can get damaged.
4. The difference between the size of the pinion and sprocket will be very large if a constant reduction is not used because of which contact angle will be very less. To overcome this we have to use idler gears which will reduce the efficiency.
5. Acceleration at the top speed is increased.

Max. Power to be transmitted:

Speed of driving Sprocket:

Vehicle Target Speed =

Static torque required to overcome static friction = $\mu \times M \times g$

[Type here]

$$= 0.4 \times 161 \times 9.81$$

$$= 631.76 \text{ N}$$

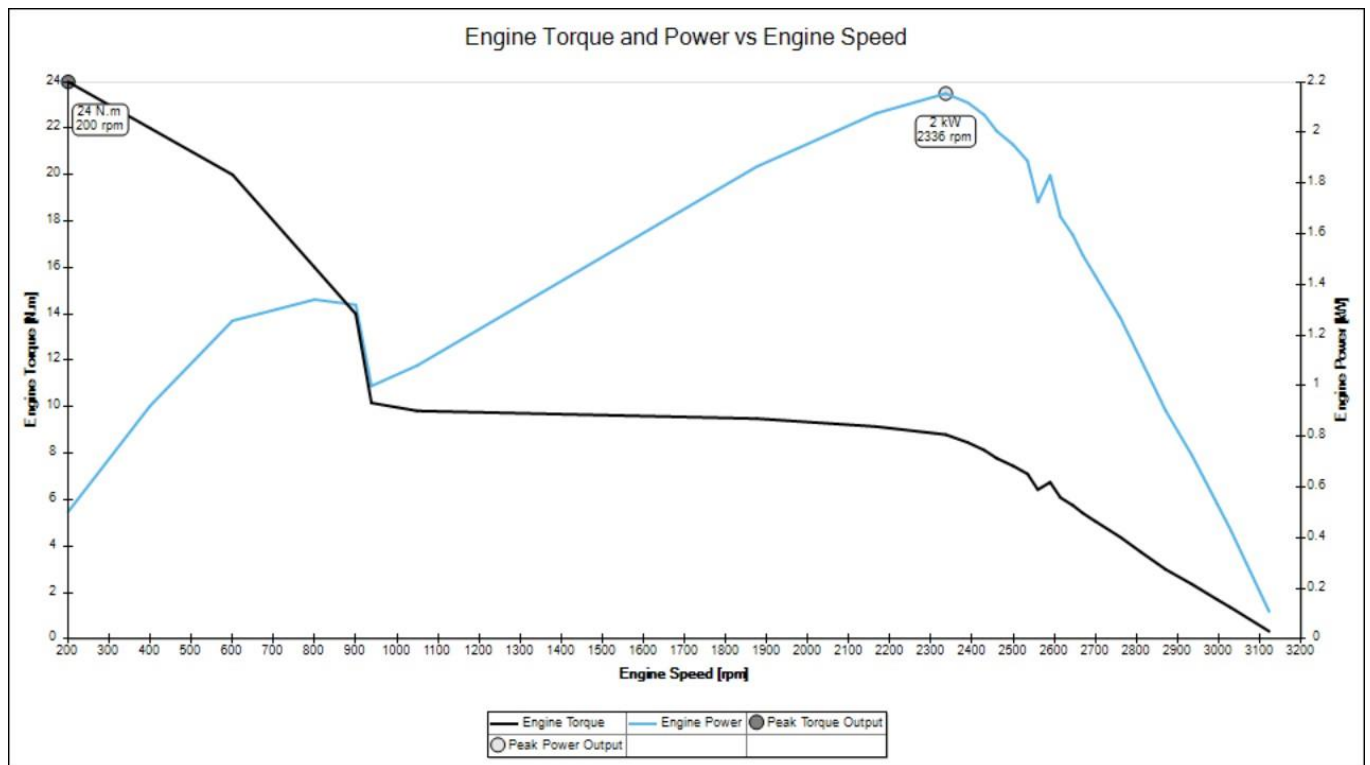
$$\text{Maximum Wheel torque required} = \text{Maximum Force} \times \text{tire radius}$$

$$= 631.76 \times 0.3$$

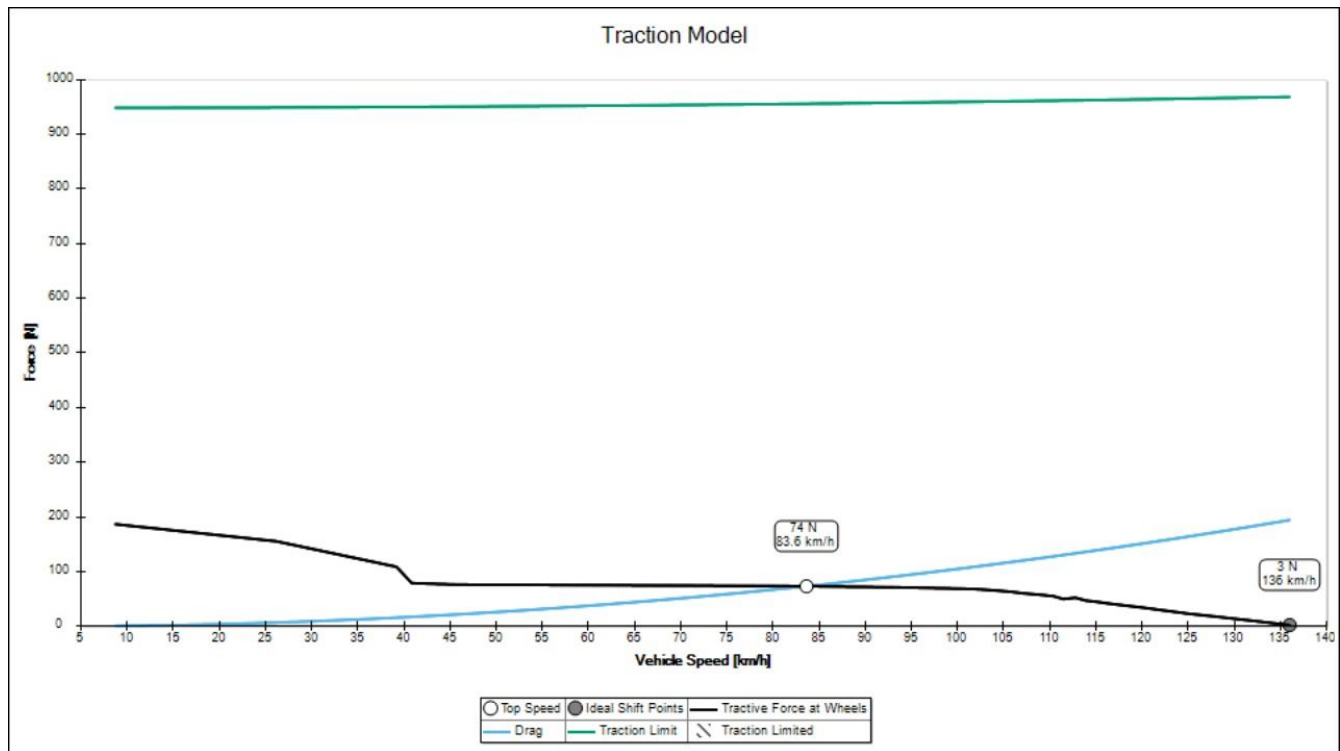
$$= 189.53 \text{ Nm}$$

Vehicle Model

- Gross mass with rider, $m = 161 \text{ kg}$
- Drag coefficient, $C_d = 0.58$
- Frontal Area, $A = 0.397 \text{ m}^2$
- Tyre Pressure, $p = 2 \text{ bar}$
- Rolling friction coefficient, $c =$
- Longitudinal friction coefficient = 1.2
- Lateral friction coefficient = 1.1
- Tire radius = 0.3m
- Transmission Efficiency = 90%
- Battery Thermal Efficiency = 90%
- Primary Drive Ratio = 1:1
- Total Gearbox Ratio = 1.265:1
- Final Drive Ratio = 2.1:1
- Battery Pack Type = Lithium



Results



- Highest Speed = 83.63 kmph
- ❖ Average Lap time = 37.80 sec
- ❖ Optimum Total Gear Reduction = 2.656
- ❖ Energy Spent = 47420 = 0.011783333 kWh

1. Transmission Design

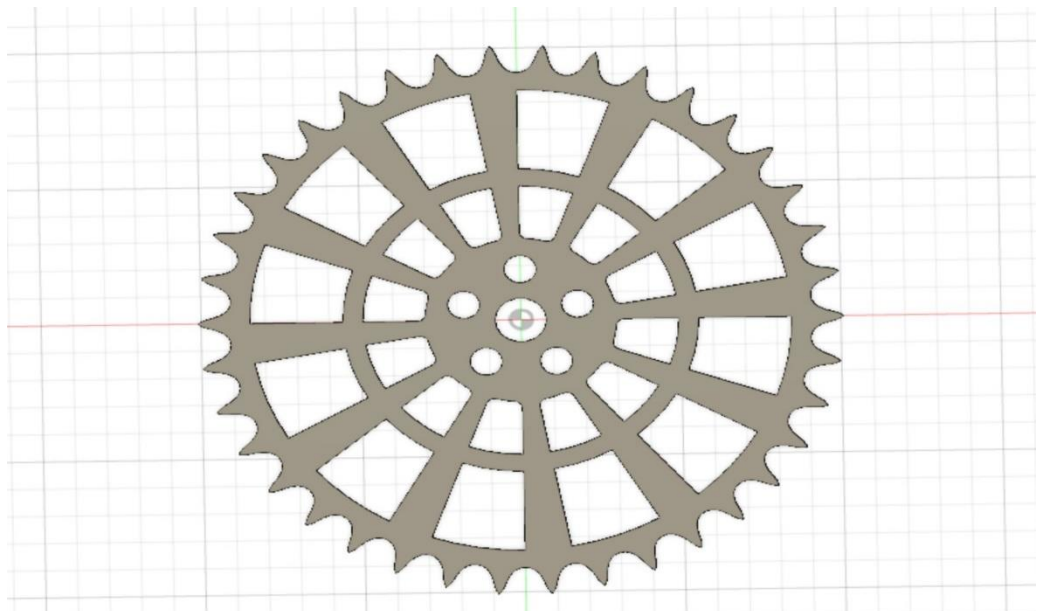
- Primary Reduction = 1:1
 - (i) Number of teeth on motor sprocket (driver) = 16
 - (ii) Number of teeth on reducer input sprocket (driven) = 16
- Gearbox reduction = 1.265 :1 Two stage reduction
 - (i) First reduction = 1.125: 1
 - a. Number of teeth on smaller gear = 16
 - b. Number of teeth on bigger gear = 18
 - (ii) Second Reduction = 1.125: 1
 - a. Number of teeth on smaller gear = 16
 - b. Number of teeth on bigger gear = 18
- Final Drive Ratio = 2.1 : 1
 - (i) Number of teeth on front sprocket = 18
 - (ii) Number of teeth on rear sprocket = 38

Powertrain Calculations

	A	B	C	D	E	F	G	H	I	J	K	L	M	N	O	P	Q	R	S	T
1	Velocity	Kerb weight	Payload	NLW																
2	V	KW	PL	NLW=KW+PL																
3	kmph	kg	kg	N	Ka	A(m2)	V2	Ra=kaAV2	a	b	Rr=(a+bV)W	Θ(rad)	sin(Θ)	Rg=Wsin(Θ)	Rt=Ra+Rr+Rg		Nrs=(V/3.6)*60/Pi/0.602			Power req
4	0	161.07	60	2168.6967	0.023	0.397	0	0	0.0012	6.03E-08	2.60243604	0	0	0	2.60243604			0		0
5	83.63	161.07	60	2168.6967	0.023	0.397	6993.977	63.862003	0.0012	6.03E-08	2.62594951	0	0	0	66.48795258			737.3687143	1.5445521	
6	80	161.07	60	2168.6967	0.023	0.397	6400	58.4384	0.0012	6.03E-08	2.62492889	0	0	0	61.06332889			705.3628739	1.3569629	
7	75	161.07	60	2168.6967	0.023	0.397	5625	51.361875	0.0012	6.03E-08	2.62352309	0	0	0	53.98539809			661.2776943	1.1246958	
8	70	161.07	60	2168.6967	0.023	0.397	4900	44.7419	0.0012	6.03E-08	2.62211729	0	0	0	47.36401729			617.1925147	0.920967	
9	65	161.07	60	2168.6967	0.023	0.397	4225	38.578475	0.0012	6.03E-08	2.62071148	0	0	0	41.19918648			573.1073351	0.7438742	
10	60	161.07	60	2168.6967	0.023	0.397	3600	32.8716	0.0012	6.03E-08	2.61930568	0	0	0	35.49090568			529.0221554	0.5915151	
11	55	161.07	60	2168.6967	0.023	0.397	3025	27.621275	0.0012	6.03E-08	2.61789988	0	0	0	30.23917488			484.9369758	0.4619874	
12	50	161.07	60	2168.6967	0.023	0.397	2500	22.8275	0.0012	6.03E-08	2.61649407	0	0	0	25.44399407			440.8517962	0.3533888	
13	45	161.07	60	2168.6967	0.023	0.397	2025	18.490275	0.0012	6.03E-08	2.61508827	0	0	0	21.10536327			396.7666166	0.263817	
14	40	161.07	60	2168.6967	0.023	0.397	1600	14.6096	0.0012	6.03E-08	2.61368247	0	0	0	17.22328247			352.681437	0.1913698	
15	35	161.07	60	2168.6967	0.023	0.397	1225	11.185475	0.0012	6.03E-08	2.61227666	0	0	0	13.79775166			308.5962573	0.1341448	
16	30	161.07	60	2168.6967	0.023	0.397	900	8.2179	0.0012	6.03E-08	2.61087086	0	0	0	10.82877086			264.5110777	0.0902398	
17	25	161.07	60	2168.6967	0.023	0.397	625	5.706875	0.0012	6.03E-08	2.60946506	0	0	0	8.316340057			220.4258981	0.0577524	
18	20	161.07	60	2168.6967	0.023	0.397	400	3.6524	0.0012	6.03E-08	2.60805925	0	0	0	6.260459254			176.3407185	0.0347803	
19	15	161.07	60	2168.6967	0.023	0.397	225	2.054475	0.0012	6.03E-08	2.60665345	0	0	0	4.66112845			132.2555389	0.0194214	
20	10	161.07	60	2168.6967	0.023	0.397	100	0.9131	0.0012	6.03E-08	2.60524765	0	0	0	3.518347647			88.17035924	0.0097732	
21	5	161.07	60	2168.6967	0.023	0.397	25	0.228275	0.0012	6.03E-08	2.60384184	0	0	0	2.832116843			44.08517962	0.0039335	

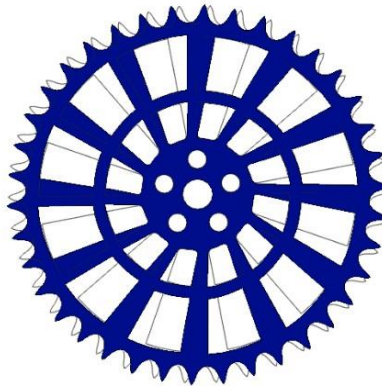
	A	B	C	D	E	F	G	H	I
1	Velocity	Load to overcome(N)	Tyre Radius(m)	Torque(Nm) = Rt*r	Nrs(RPM)	FDR	Nrs(rad/s)	Npinion	Driving Power (T*rad/s)
2	V								
3	83.63	125.4113504	0.307	38.50128457	#####		2 77.177926	1474.7374	2971.449279
4	80	118.7281683	0.307	36.44954766	#####		2 73.827981	1410.7257	2690.996513
5	75	109.9166859	0.307	33.74442257	#####		2 69.213732	1322.5554	2335.577428
6	70	101.5617535	0.307	31.17945834	#####		2 64.599483	1234.385	2014.176902
7	65	93.66337118	0.307	28.75465495	#####		2 59.985235	1146.2147	1724.854723
8	60	86.22153882	0.307	26.47001242	#####		2 55.370986	1058.0443	1465.670681
9	55	79.23625646	0.307	24.32553073	#####		2 50.756737	969.87395	1234.684565
10	50	72.7075241	0.307	22.3212099	#####		2 46.142488	881.70359	1029.956163
11	45	66.63534174	0.307	20.45704991	#####		2 41.528239	793.53323	849.5452649
12	40	61.01970938	0.307	18.73305078	352.681437		2 36.913991	705.36287	691.5116589
13	35	55.86062702	0.307	17.1492125	#####		2 32.299742	617.19251	553.915134
14	30	51.15809466	0.307	15.70553506	#####		2 27.685493	529.02216	434.8154793
15	25	46.9121123	0.307	14.40201848	#####		2 23.071244	440.8518	332.2724834
16	20	43.12267994	0.307	13.23866274	#####		2 18.456995	352.68144	244.3459355
17	15	39.78979758	0.307	12.21546786	#####		2 13.842746	264.51108	169.0956243
18	10	36.91346522	0.307	11.33243382	#####		2 9.2284976	176.34072	104.5813387
19	5	34.49368286	0.307	10.58956064	#####		2 4.6142488	88.170359	48.86286763

Rear Sprocket Design



☐ **Safety Factor (Per Body)**

0  8



Name	Minimum	Maximum
Safety Factor		
Safety Factor (Per Body)	15	15
Stress		
Von Mises	0.001304 MPa	10.68 MPa
1st Principal	-2.156 MPa	12.69 MPa
3rd Principal	-12.65 MPa	2.065 MPa
Normal XX	-11.85 MPa	11.01 MPa
Normal YY	-11.59 MPa	12.1 MPa
Normal ZZ	-2.938 MPa	2.883 MPa
Shear XY	-5.568 MPa	5.288 MPa
Shear YZ	-0.8298 MPa	0.9043 MPa
Shear ZX	-0.8827 MPa	0.9443 MPa
Displacement		
Total	0 mm	0.005758 mm
X	-0.005338 mm	0.00551 mm
Y	-0.005734 mm	0.004854 mm
Z	-4.457E-05 mm	5.137E-05 mm
Reaction Force		
Total	0 N	27.35 N
X	-22.83 N	17.8 N
Y	-19.32 N	24.87 N
Z	-1.884 N	2.077 N
Strain		
Equivalent	7.271E-09	8.552E-05
1st Principal	-2.9E-09	8.95E-05
3rd Principal	-8.83E-05	-5.646E-09
Normal XX	-4.978E-05	4.737E-05
Normal YY	-4.839E-05	5.025E-05
Normal ZZ	-1.27E-05	1.381E-05
Shear XY	-7.155E-05	6.796E-05
Shear YZ	-1.066E-05	1.162E-05
Shear ZX	-1.134E-05	1.213E-05

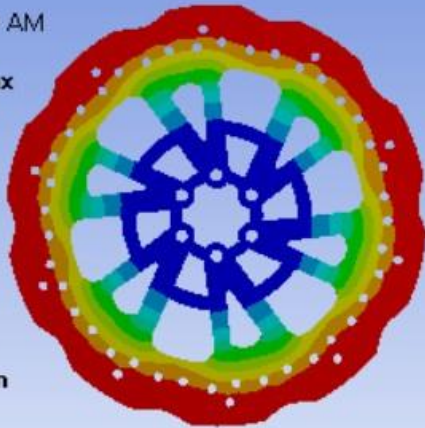
Static Stress Analysis

Front Disc

B: Steady-State Thermal

Temperature
Type: Temperature
Unit: °C
Time: 1
9/22/2021 12:31 AM

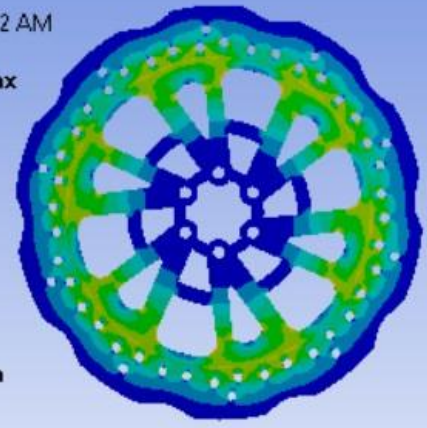
48.877 Max
46.056
43.234
40.413
37.591
34.77
31.948
29.126
26.305
23.483 Min



B: Steady-State Thermal

Total Heat Flux
Type: Total Heat Flux
Unit: W/m²
Time: 1
9/22/2021 12:32 AM

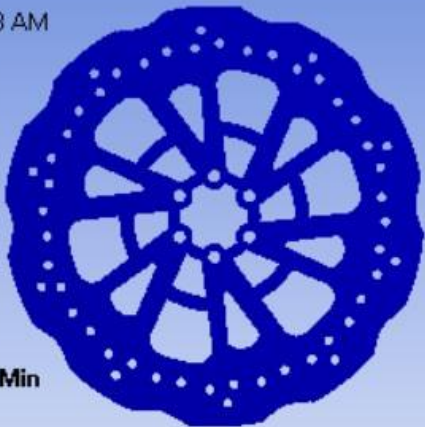
45183 Max
40163
35144
30124
25104
20085
15065
10045
5025.8
6.099 Min



C: Static Structural

Life
Type: Life
9/22/2021 12:33 AM

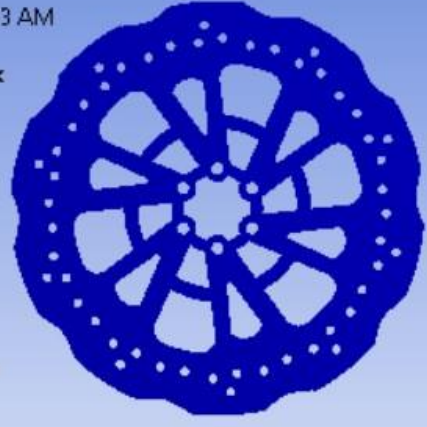
1e6 Max
9.3759e5
8.7908e5
8.2422e5
7.7278e5
7.2455e5
6.7934e5
6.3694e5
5.9719e5
5.5992e5 Min



C: Static Structural

Damage
Type: Damage
9/22/2021 12:33 AM

1786 Max
1674.5
1570
1472
1380.2
1294
1213.3
1137.6
1066.6
1000 Min



Aerodynamics

Aerodynamics is the study of how gases interact with stationary or moving bodies. In a motorbike, the fairing is an external shell placed over the frame which is the primary way to streamline the vehicle, eventually reducing air drag and getting a desired value of downforce, and to model a perfectly manufacturable Fairing.

AERODYNAMIC FORCES AND DEFINITIONS-

Drag and Lift are the two primary aerodynamic forces acting on the vehicle.

1) Drag Force-

Drag is the force that is acting opposite to the relative motion of any object moving with respect to a surrounding fluid. The following is the formula for calculating drag-

Drag Force = $(\frac{1}{2}) \rho V^2 C_D A$ Where,

‘ ρ ’ is Density of the fluid (Air to be specific) ‘ v ’ is the Flow velocity of the object

‘ C_D ’ is the Coefficient of Drag ‘ A ’ is the Frontal Area

2) Lift Force-

Lift is the component of force that is perpendicular to the oncoming flow direction. The following is the formula for calculating lift-

Lift Force = $(\frac{1}{2}) \rho V^2 C_L A$ Where,

‘ ρ ’ is Density of the fluid (Air to be specific) ‘ v ’ is the Flow velocity of the object

‘ C_L ’ is the Coefficient of Drag ‘ A ’ is the Frontal Area

SIMULATION RESULTS AND DISCUSSION-

Air Flow Simulation and Post processing-

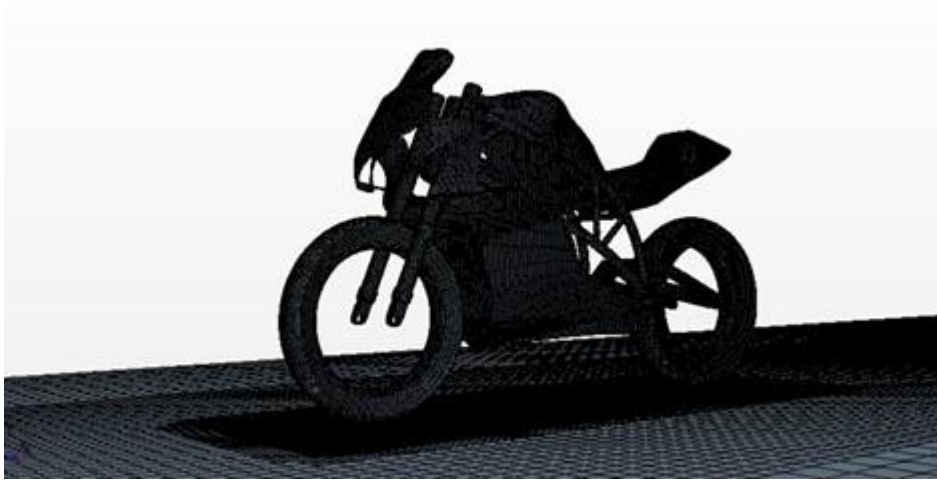
Improvement in the aerodynamics and aesthetics of the motorcycle was done using Star CCM+. The modelling of the fairing CAD was done to be easily rendered in CFD simulation interface of STAR CCM+. Some of the complex parts like Swingarm, BMS, the components of motor, as well as the rider have been replaced by simple geometric shapes that resemble the actual structure of the parts and would not have any changes on the results obtained after post processing of the Air flow simulation.

As per the simulation setup, the maximum velocity was taken as 23.23 m/s. The fairing contributes a frontal area of 0.356 m^2 for the final iteration. In the simulation setup, the reference pressure was considered to be 101.325 KPa and the reference density of air is taken to be 1.18415 kg/m^3 .

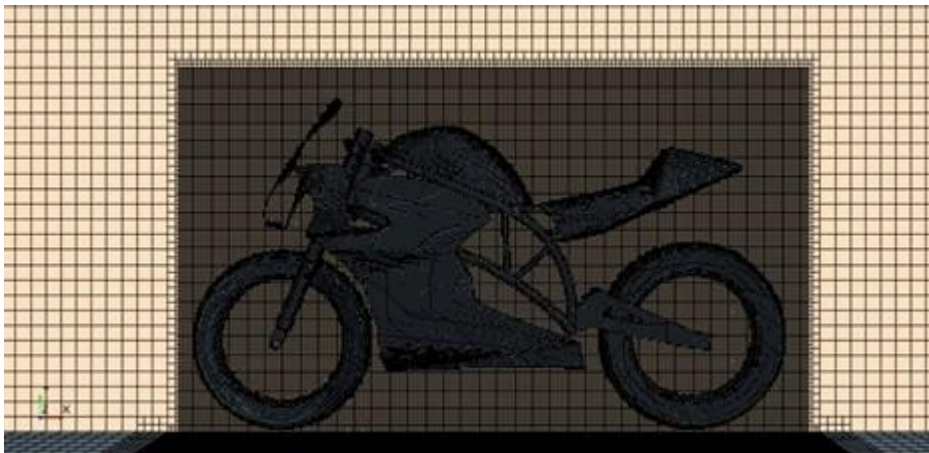
The first iteration of the CAD was simulated and on the basis on the results obtained, the second iteration was designed. The results of both the iterations have been compared. The values of air density and reference pressure were kept constant. From the table below we can observe that the frontal area was reduced in Iteration 2, which in turn has had a positive impact on the Forces and their respective coefficient. The negative sign, accompanying the lift force and lift force coefficient shows that the lift is negative which means that it is a downforce, and is most desirable.

	<u>ITERATION 1</u>	<u>ITERATION 2</u>
1) Frontal Area (m^2)	0.397	0.356
2) Drag Force (N)	76.99	66.41
3) Lift Force (N)	12.68	-12.816
4) Coefficient of Drag (C_D)	0.607	0.5838
5) Coefficient of Lift (C_L)	-0.10	-0.1126

MESHING VERSIONS AND POST PROCESSING-

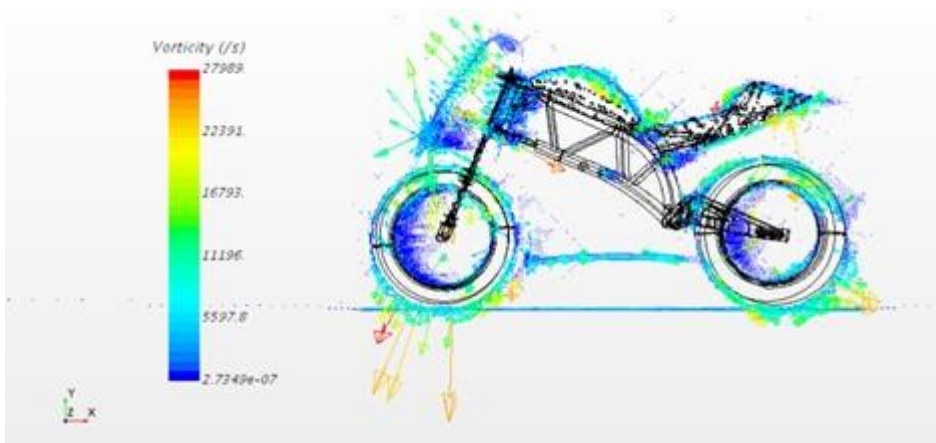


Trimmer Mesh Tool results

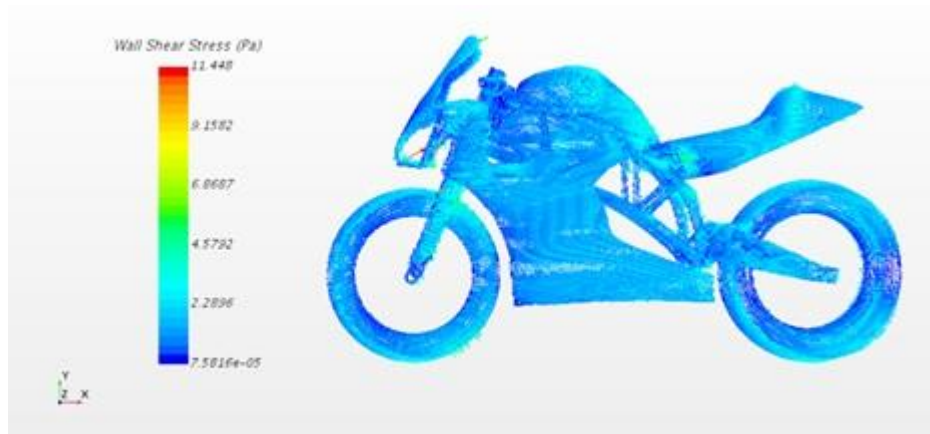


Meshing of the Fluid Domain and the Motorbike under Volume Mesh Scene

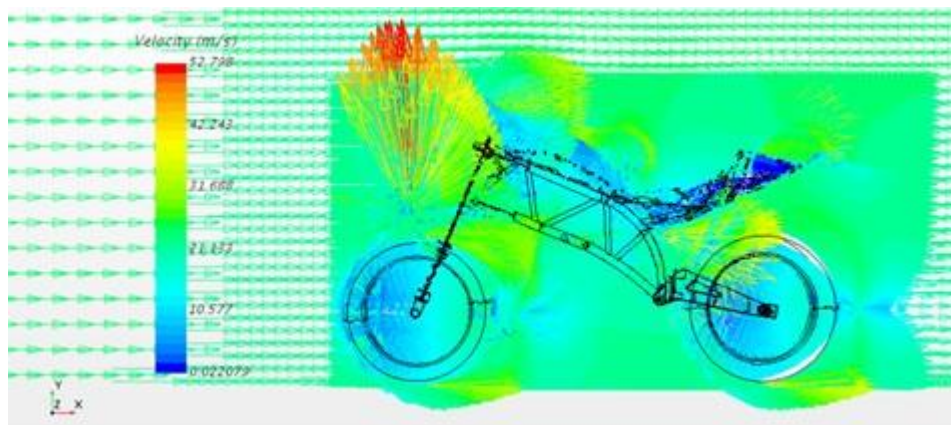
POST PROCESSING IN STAR CCM+ INTERFACE-



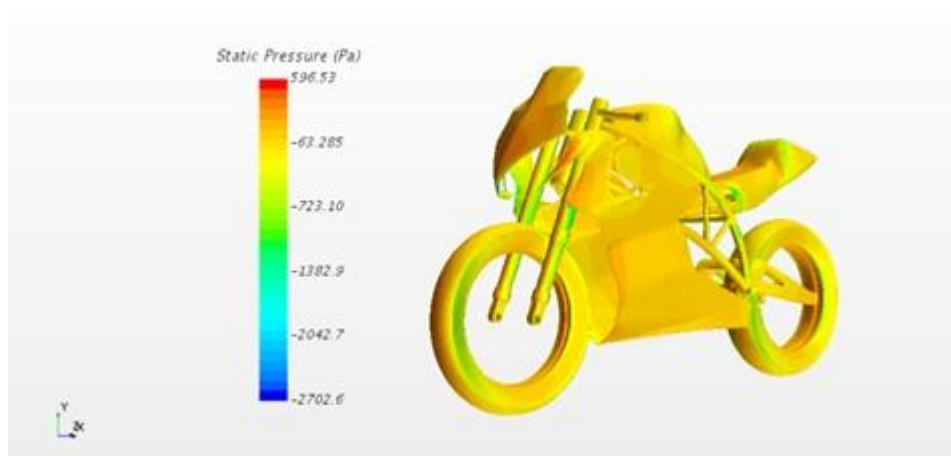
Vorticity Plot for a Section Plane passing through the CAD



Wall Shear Stress on the Surface of Motorbike under Vector Scene



Velocity Plot on the Surface of Motorbike under Vector Scene



Static Pressure Contour under Scaler Scene